Novel bioresorbable phosphate glass fiber textile composites for medical applications

*Chenkai Zhu [ab], Ifty Ahmed [c], Andrew Parsons [d], Yunqi Wang [ab], Chao Tan [ab], Jingsong Liu [e], Chris Rudd [abd], Xiaoling Liu [ab]**

a. *Ningbo Nottingham International Academy for the Marine Economy and Technology, The University of Nottingham Ningbo China, Ningbo, 315100, China*

b. *Ningbo Nottingham New Materials Institute, The University of Nottingham Ningbo China, Ningbo, 315100, China*

c. *Advanced Materials Research Group, Faculty of Engineering, University of Nottingham, Nottingham, NG7 2RD, UK*

d. *Composites Research Group, Faculty of Engineering, University of Nottingham, Nottingham, NG7 2RD, UK*

e. *Department of Technology, Sinoma Co., Ltd.,198 Tongtian Road, Nanjing, 211100, China*

* *Corresponding author at: Room 445, Science and Engineering Building, The University of Nottingham Ningbo China, Ningbo, 315100, China.*

Tel: +86 (0)574 8818 0000 (ext 8057)

Email address: Xiaoling.Liu@nottingham.edu.cn

Abstract

A manual bench-top inkle-type loom was designed to enable hand woven textiles. These PGF textiles, along with unidirectional (UD) fiber mats made from the same batch of yarns, were utilized to manufacture fully resorbable textile composites (T-C), unidirectional aligned fiber composites (UD-C) and 0 ⁄90 ° lay-up UD fiber reinforced composites (0/90-C). The fiber volume fraction in the composites was set at ~20%. Retention of flexural properties and mass loss of the composites were evaluated during degradation in phosphate buffered saline (PBS) at 37 ℃ for 28 days. The higher flexural strength and modulus values observed for the T-C when compared to 0/90-C were attributed to the textile weaving resulting in a biased fabric with a higher density of fibers in the warp direction. After 28 days immersion in PBS ~20% flexural strength and ~25% flexural modulus values for the UD-C, T-C and 0/90-C composites were still prevalent.

Keywords*: Fibers; Composite; Mechanical Properties; Degradation.*

Introduction

Traditional implants used for bone fracture repair in load-bearing situations have usually been made using metal materials. This is to ensure sufficient mechanical support and includes stainless-steel, Cr-Co and Ti alloys [1-3]. Metallic implants cannot adapt to changing physiological properties [4, 5]. The high stiffness of metallic bone plates is known to result in "stress shielding" effects [5-7], whereby the majority of the load is carried by the plate rather than by the underlying bone. This causes resorption of the unloaded bone tissue, with the possibility of a resulting fracture at the same site after removal of the plate [8-10]. Additionally, they can have the disadvantage of requiring removal via second surgery following fracture healing [11].

Biodegradable polymers such as polylactic acid (PLA) exhibit good cytocompatibility and their degradation behavior has been heavily explored for biomedical applications [12-14]. However, the relatively low stiffness properties of PLA render it incapable for use in load-bearing conditions [15, 16]. To achieve sufficient modulus for load-bearing bone repair applications, composites have been investigated that are based on biodegradable polymers with a bioactive reinforcement phase [17-20].

After the first introduction of bioactive glasses by Hench et al, bioactive glasses have been a growing interest for implant application with ability to form a direct bond to living bone by forming a surface hydroxyapatite layer in physiological conditions [21-23]. There are now several types of bioactive glasses, including conventional silicate glass [24-26], phosphate based glass [27-30] and borate based glass [31-33].

As the limited mechanical strength and low toughness prevented application of bioactive glasses, composite optimized properties, combining the polymer and fibers with has long

been a goal [23]. Currently, phosphate based glasses (PBG) have been a potential inorganic reinforcement phase that have been investigated to produce composites that are fully degradable. Phosphate based glasses (PBG) offer variable degradation rates as their solubility can be tailored through altering their chemical composition [34]. In addition, their polymeric structure allows them to be drawn into continuous fibers to provide improvements in strength [20, 35]. The ionic components of the glass released during degradation could provide both support for bone growth (i.e calcium and phosphate ions) along with other required trace elements to promote fracture site healing [36].

Ahmed et al [37] and Felfel et al [38] investigated PLA composites (18%V_f) reinforced with random and unidirectional (UD) iron doped PGF and reported that the flexural strength values of random and UD composites were 106 MPa and 115 MPa whilst the modulus values were 6.7 GPa and 9 GPa respectively. More recently, phosphate based glass fibers with addition of 5-10% B_2O_3 presented significant improvement of mechanical properties (~1000 MPa of tensile strength and ~12 GPa of Young's Modulus) [39-41]. As such, it was reported that borophosphate glass fiber reinforced UD PLA composites (with 20% V_f) could achieve values of ~156 MPa and ~12 GPa for flexural strength and flexural modulus [41], providing mechanical properties similar to those of cortical bone [4].

Due to difficulty in fiber forming, phosphate glass fibers are mostly produced only in single filament form in lab-scale quantities [17, 29, 37, 42-45]. Composites produced using hand layup of UD fibers have limitations in terms of fiber alignment, are time consuming to make and are not easily scalable. However, as the textile fabric is a well-utilized form of reinforcement in the composites industry, developing phosphate glass

fibers into textile forms is the prerequisite condition, significant facilitating eventual industrial production [46].

Due to success of developing PBG formulations that were both suitable for scaled-up fiber production and also cytocompatible [47, 48]. The PBG formulation $48P_2O_5$-$12B_2O_3$-14CaO-20MgO-$1Na_2O$-$5Fe_2O_3$ in particular presented excellent scale-up manufacture capability and was used to produce multifilament twisted yarns of PGF suitable for weaving. Based on this glass, Wang et al [49, 50] has developed Inkle loom for textile weaving and successfully produced the first ever woven textile fabric of PGF. This study made use of these yarns to produce the pure PGF textile fabrics using the Inkle loom developed by them [49, 50]. The effectiveness of these textiles was then assessed by incorporating them into fully resorbable PGF/PLA composites. In order to compare mechanical properties with a textile reinforced composite, a 0 ⁄90 ° unidirectional lay-up composite was also fabricated as a pseudo-zero crimp textile composite. The retention of flexural properties and weight loss of the composites was evaluated during immersion in PBS at 37 ℃ for up to 28 days.

Materials and methods

Preparation of fiber products for textile manufacture

In this study, phosphate based glass fiber products used for UD mats and textile weaving utilizing yarns of phosphate glass fiber were made at industrial scale in Sinoma Co. Ltd (China). The glass formulation was $48P_2O_5$-$12B_2O_3$-14CaO-20MgO-$1Na_2O$-$5Fe_2O_3$ and the fibers were coated with water-soluble epoxy when fibers were drawn from the bushing. The size was designed by Sinoma Co. Ltd (China), to improve fiber surface quality and

combine fibers together as a strand for yarn twisting. However, as it is commercially confidential, the composite of size used in this study cannot be presented. The manufacturing process for yarn products is different from roving due to the application of a twist, which can provide additional integrity to the yarn before it is subjected to the weaving process [51, 52]. Yarn production in this study was accomplished by twisting together two 50-filament strands (with S twist type) to be one pre-twist yarn, then re-twisting four pre-twist yarns (with Z twist type) to be balance twisted yarn (eight strands). This process was finished using a twisting machine (TKV216 Type, Tianchen, China) with inserted twist of 55 tpm (twist per meter).

Design and manufacture of Inkle-type loom for textile fabrication

Theoretically, textile fabrics are produced by the interlacing of warp (longitudinal) and weft (traverse) fibers in a regular pattern or weave style. The integrity of the fabric is maintained via mechanical interlocking of the fibers [46]. The Inkle-type loom for

textile weaving in this study was produced in-house and was presented in

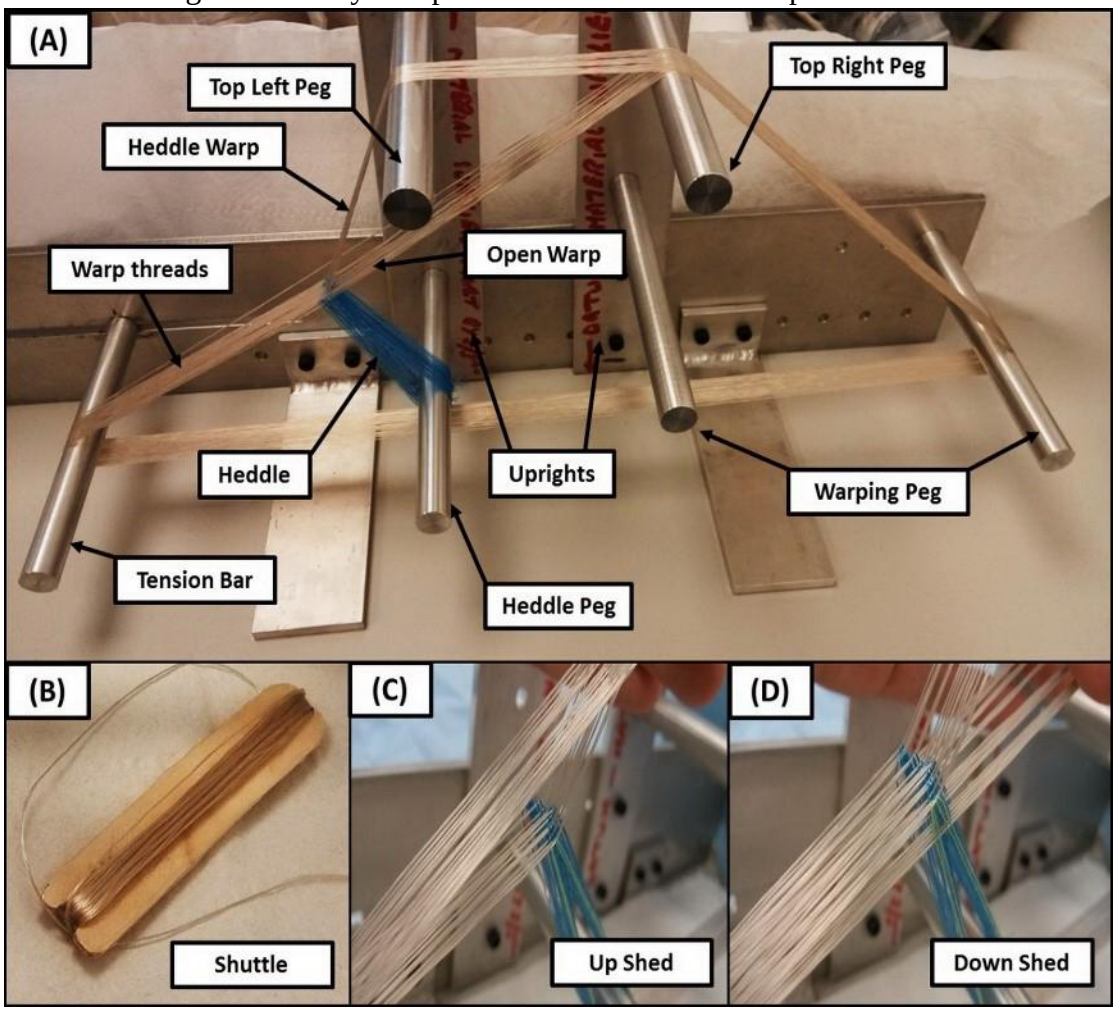

Figure *1*. The surface of all pegs fixed on uprights and the surfaces of the tension bars were all polished in order to reduce the friction effect on the surface of the warp yarns.

During the weaving process, the yarns were wound onto the inkle-type loom to produce a warp. The end of the yarn was fixed onto the tension bar, then taken up from tension bar, over the two top pegs and the warping peg, then returned around the tension bar. The yarn was then wrapped around again, but this time by passing under the top left peg. The warp was built up by alternating wrapping in this way until a warp of sufficient width was produced.

A “heddle” was used to bring the two sets of warp yarns into alignment. String was used to pull the upper warp yarns down so that they lay next to the lower yarns (see

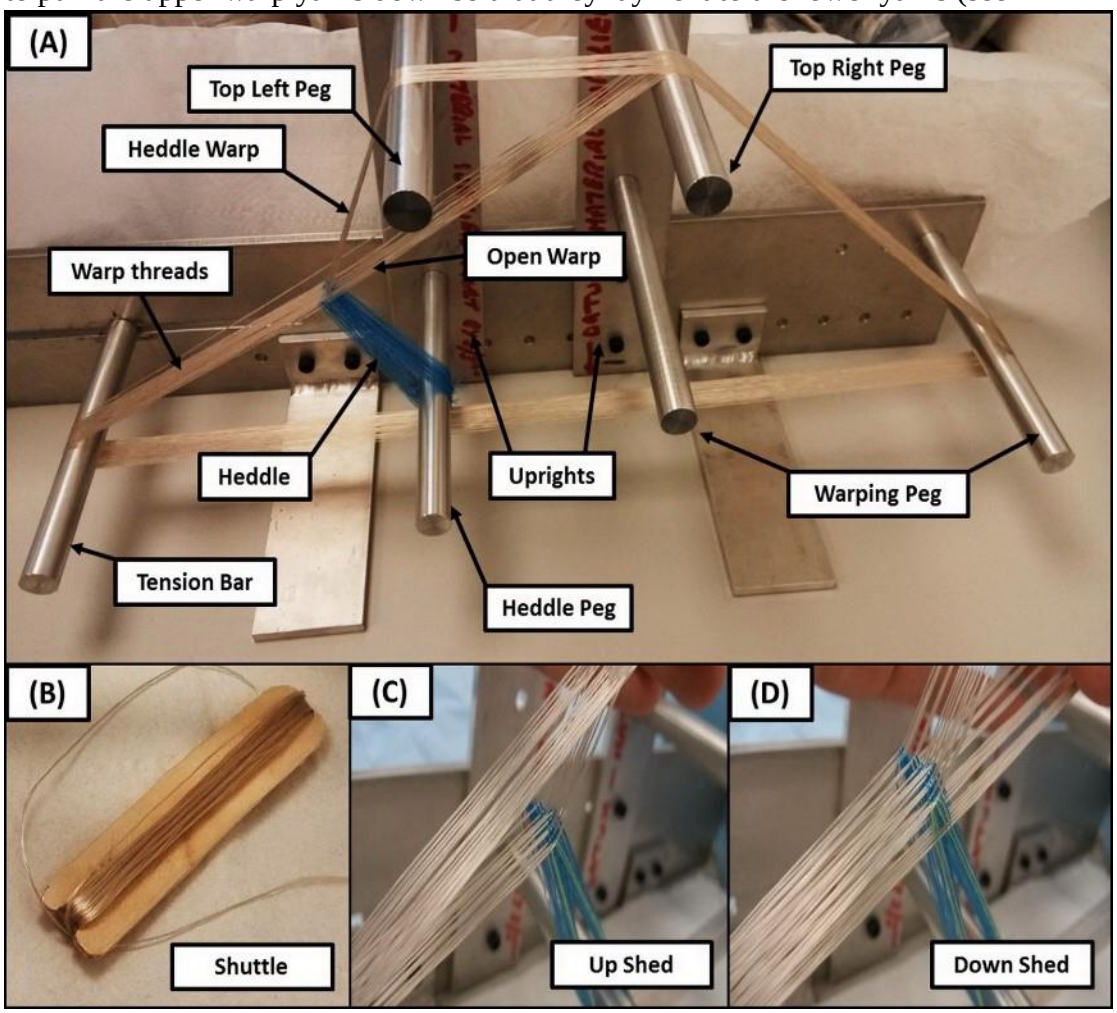

Figure *1* A). The yarns that were pulled down by the strings were called the “heddle warp”, whilst the yarns not pulled down by the string were called the “open warp”. The

open warp could be raised or lowered

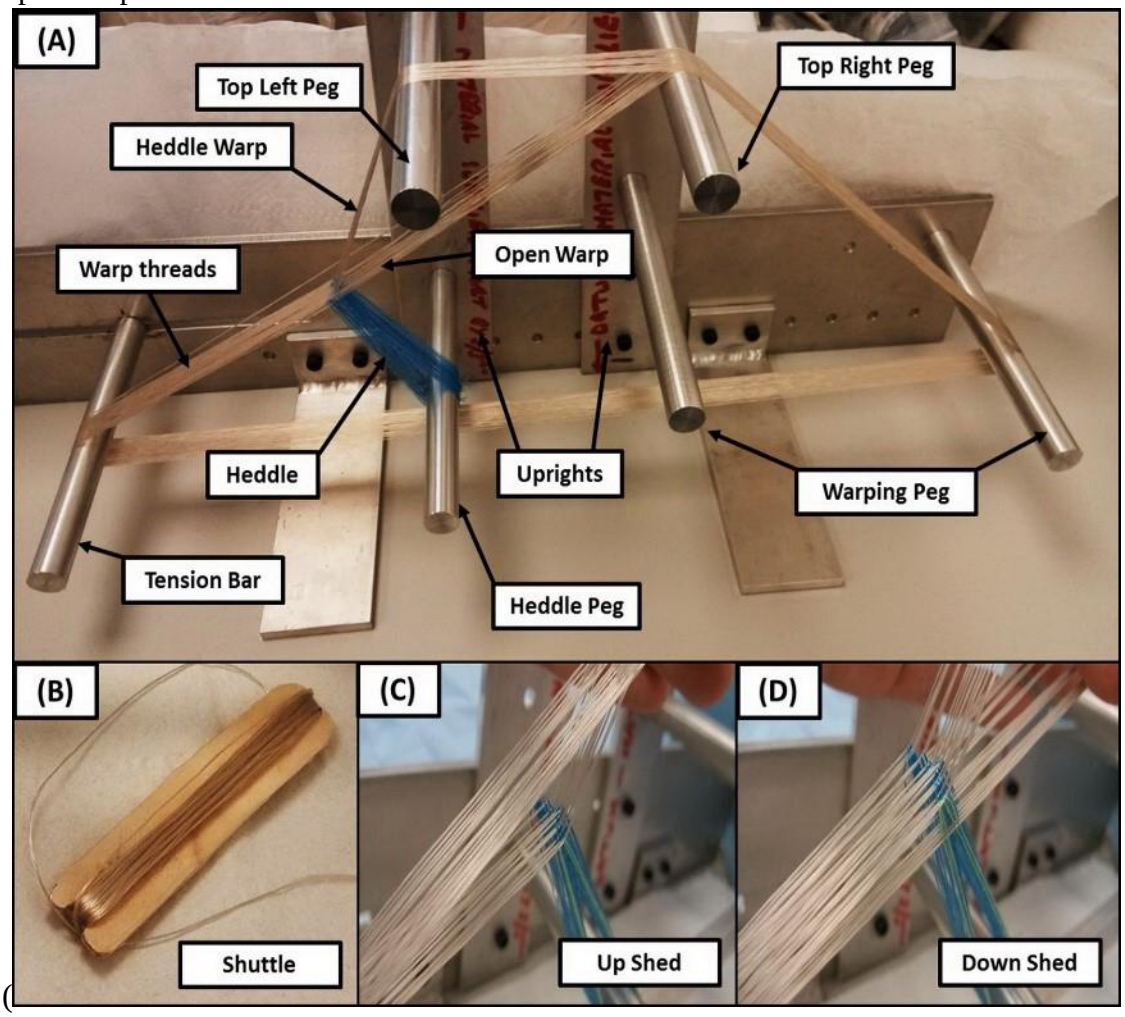

(

Figure *1* C and D) to create an opening called a shed. The shuttle

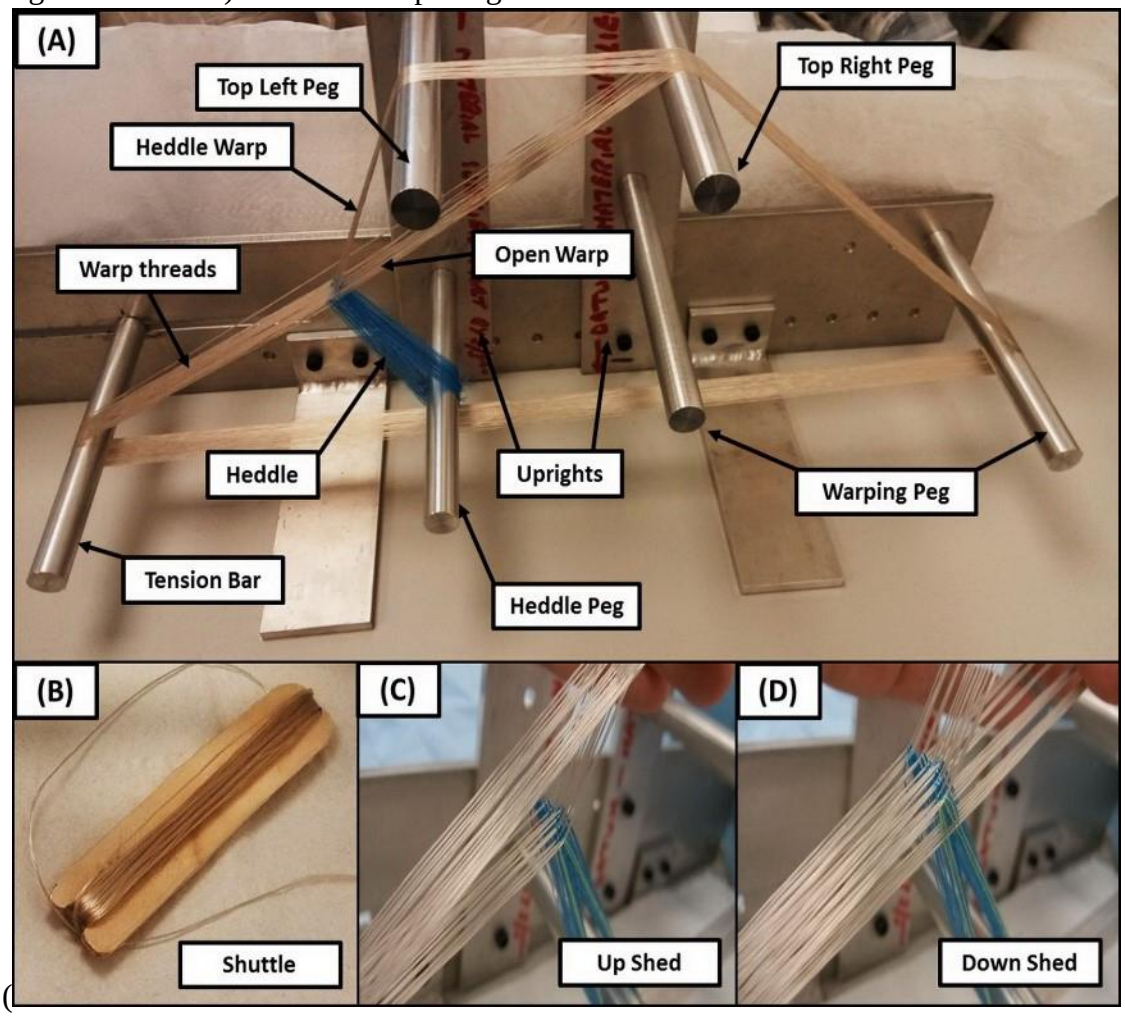

(

Figure *1* B) was then used to guide weft yarns through the shed. The tension bar was adjusted to keep the warp under tension when weaving.

During weaving, the shuttle was passed through the shed from left to right as the open warp was lifted up and down. The resulting textile fabric was a plain weave, with each

warp and weft yarn passing over and under each other, as shown in

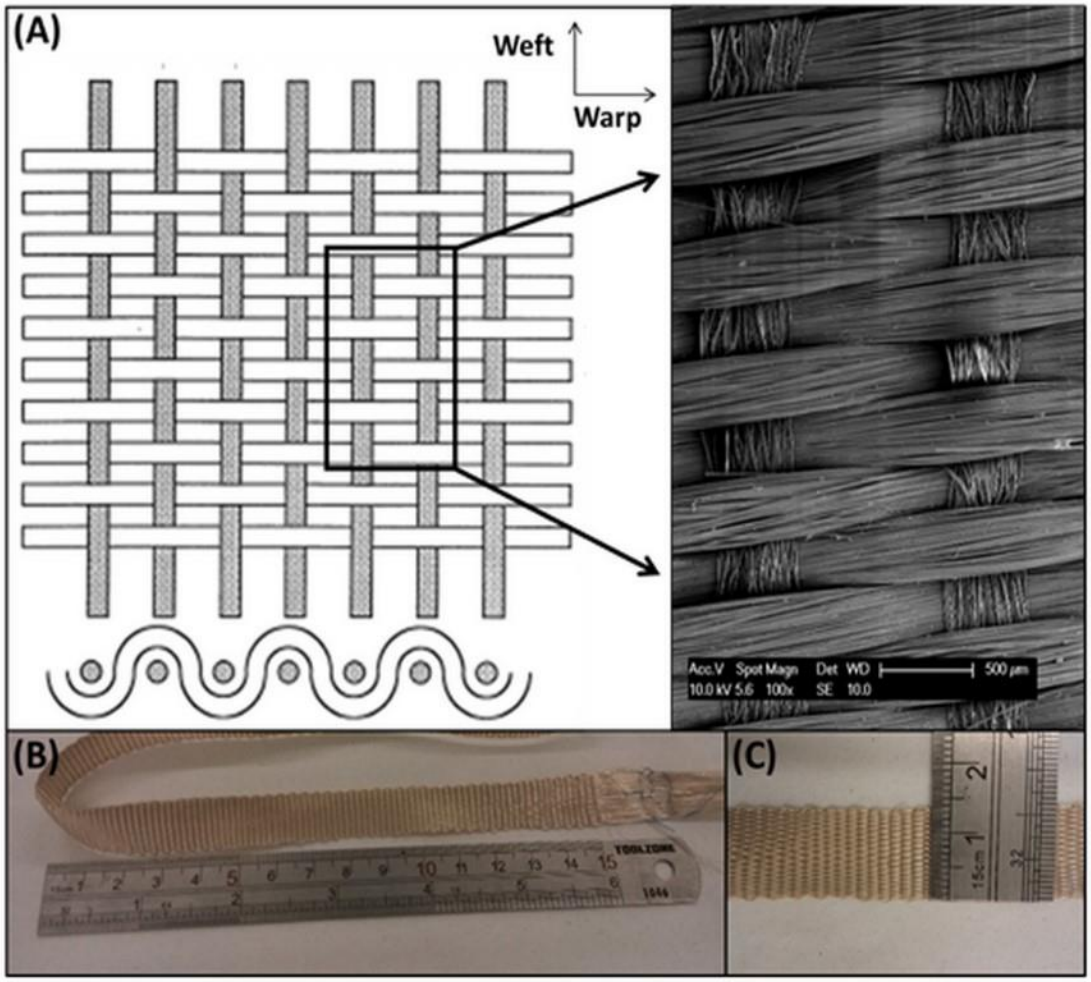

Figure 2. Details of the parameters of the textiles are listed in Table 1.

Preparation of unidirectional fiber mats

Unidirectional (UD) fiber mats were produced from yarns of glass fiber. The yarns were rewound and aligned using a 310 mm diameter drum with a Polytetrafluoroethylene (PTFE) cover sheet. A solution of PLA (3251D NatureWorks®, UK) was prepared by adding PLA granules to chloroform (Sigma-Aldrich, UK) at a concentration of 0.05g/ml. An aerosol method was then used to spray this PLA solution onto the yarn on the drum.

The drums were then left in a fume hood for 2 hours in order to allow the solvent to evaporate. The resulting UD fiber sheets were removed from the drum and cut into sections (140 × 128 mm^2) for composite production, based on the size of the mold.

Poly-lactic acid film production

PLA films (0.2 mm thickness) were prepared by compression molding PLA pellets (3251D, NaturalWorks, UK), which had been dried in a vacuum oven at 50 ℃ for 24 hours. The PLA pellets (5g) were put between two aluminum plates and placed into a downstroke press (160 TD/S, Daniels, UK) at 210 ℃ for 10 minutes of pre-heating, followed by 1 min pressing at 0.5 MPa. The plates were then moved into an upstroke press (M-B1, Mackey Bowley, UK) for 5 minutes of cooling under pressure 0.5 MPa.

Manufacture of composites

As can be seen in

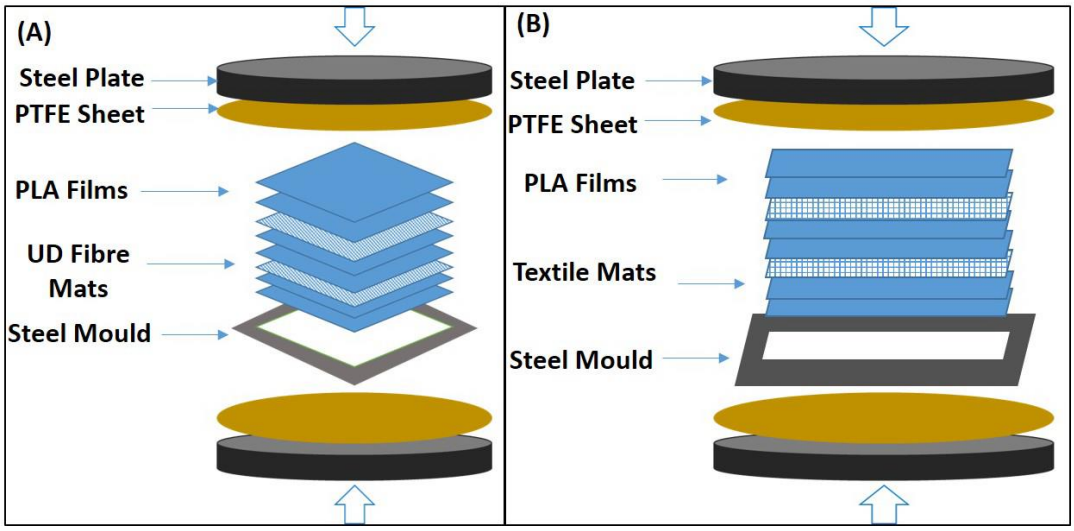

Figure 3 A, the unidirectional fiber mat reinforced composites (UD-C) and 0 °/90 ° lay-up composite (0/90-C) were produced via a film stacking process by using a 140 × 128 × 2 mm^3 steel mold where the fibre mats and PLA film were placed in the mold layer by layer. For the 0 °/90 ° lay-up, UD fiber mats and PLA film were balanced laid alternately in the longitudinal direction (0 °) and traverse direction (90 °). The total mass of fiber mats and PLA film were calculated based on the composite fiber volume fraction (V_f), density of glass fiber, density of PLA and volume of composite. The filled mold was placed into a downstroke press (160 TD/S, Daniels, UK) and pre-heated at 180 ℃ for 10 min, followed by 10 min pressing at 4 MPa. The mold was then moved to a upstroke press (M-B 1, Mackey Bowley, UK) and held under a pressure of 3.5 MPa while cooling to room temperature.

The textile reinforced composites (T-C) were manufactured via a film stacking process in a similar fashion to the UD-C composite. Due to the limitations of the textile manufacturing technique, the size of the textile fabric was 140 × 15 mm^2, thus a new steel mold of 140 × 15 × 2 mm^3 was produced for textile reinforced composite manufacture (see

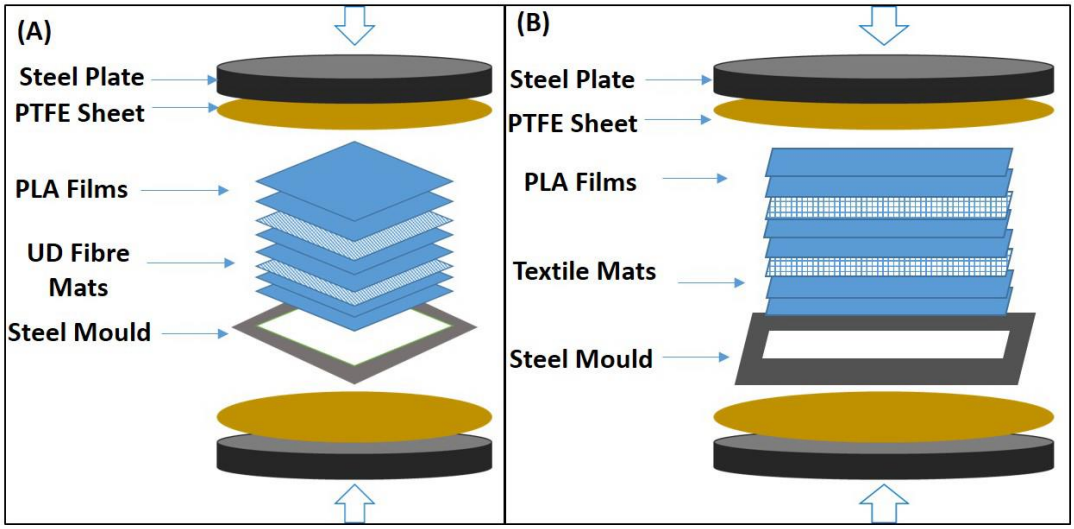

Figure 3 B).

A control, neat PLA plate was produced by filling the mold with an appropriate number of PLA films and following the same heating and pressing procedure, so as to ensure a comparable processing history. The fiber/PLA plates were cut to the required dimensions for characterization by a band saw.

Fiber mass and volume fraction

The fiber mass and volume fraction of the composites were obtained using the matrix burn off method, based on the standard test method ASTM D2584-11 [53]. Triplicate composites samples were placed individually into pre-weighed metal trays, with the total masses of sample and tray then weighed before being put into a furnace equipped with an afterburner. The samples were held at 450 °C for 3 hours in order to allow for the complete combustion of the PLA. The weight of the tray and remaining fibers was then weighed. The fiber mass fraction (W_f) was calculated according to Equation 1.

$$W_f = \frac{m_{ca} - m_{tr}}{m_{cb} - m_{tr}} \times 100\% \qquad \text{Equation 1}$$

Where W_f is the fiber mass fraction, m_{tr} is the mass of metal tray, m_{cb} is the mass of metal tray within samples before burn off, m_{ca} is the mass of metal tray within samples after burn off.

The fiber volume fraction (V_f) was calculated as follows,

$$V_f = \frac{(m_{ca} - m_{tr})/\rho_f}{[(m_{cb} - m_{ca})/\rho_{PLA}] + [(m_{ca} - m_{tr})/\rho_f]} \times 100\% \qquad \text{Equation 2}$$

Where V_f is fiber volume fraction, ρ_f is the density of glass fiber and ρ_{PLA} is the density of PLA.

In this study, the densities of the PLA matrix and phosphate glass fiber reinforcement were: ρ_{PLA} = 1.24g mm^{-3} (PLA 3251D), ρ_f = 2.67 g mm^{-3} respectively [28].

In vitro degradation study

The specimens of composites and neat PLA plates were immersed in 30 ml phosphate buffered saline (PBS) solution in glass vials, according to the standard BS 10993-13:2010 [54]. Eight time points were considered and the specimens were extracted and weighed after blot drying with tissue. The PBS solution was changed at each time point. Measurement of mass loss, pH value and water uptake were recorded at each time point.

Flexural properties test

Flexural tests (three point bending) were used to determine initial flexural strength and modulus values. The tests were conducted in accordance with BS 14125:1998 [55] using an ElectroForce® (3330 series, Bose, USA). The sample dimensions were 40 × 15 × 2 (l×b×h) mm with a 32 mm test span. A cross-head speed of 1 mm min^{-1} was used with a 3 KN load cell. The samples were positioned such that the fiber direction was along the span (i.e. a 0 °orientation). The measurement was carried out in triplicate.

SEM observation

After flexural testing, the composite samples were cooled in liquid nitrogen for 1 minute and fractured manually. Care was taken to ensure that the fracture was created outside the zone of damage from the flexural testing. After sputter coating with platinum, the cross-section of the freeze-fractured composite was examined by using a Philips XL30 (Oxford, UK) scanning electron microscope operated at 10 KV.

Crystallinity Analysis

Crystallinity of PLA polymer of composite and PLA plate was analyzed using a DSC Q10 (TA Instrument, USA). Small specimens (around 10 mg) from the composite and PLA plates were placed into aluminum plans and heated from 20 to 200 ℃ at a heating rate of 10 ℃ mm^{-1} under a nitrogen gas stream at 50 ml min^{-1}. A blank pan measurement was used for the baseline measurement and at least three samples were tested for each sample type. The percentage crystallinity (X_c) of PLA was calculated according to Equation 3 [38, 56]:

$$X_c\% = \frac{(\Delta H_m - \Delta H_c)}{\Delta H_m^0 \cdot X_p\%} \qquad \text{Equation 3}$$

Where ΔH_m and ΔH_c are the melting and the crystallization enthalpies, respectively. The X_p is the mass fraction of PLA matrix and the ΔH_m^0 is the reference ΔH_m for PLLA crystals with an infinite size (taken to be 93.6 J g^{-1}) [57].

Statistical analysis

The average values and standard error of all data involved in this paper were calculated and analyzed using the Prism software (version 6.0, GraphPad Software, San Diego, CA, USA). A one-way analysis of variance (ANOVA) was calculated with the Tukey multiple post-test to compare the significance of change in one factor with time. The error bars on all the data represent standard error of mean.

Results

Fiber volume fraction and initial flexural properties

The fiber volume fractions of the composites were ascertained by burn off tests and are listed in Table 2. There was no significant difference (P>0.05) amongst experimental fiber volume fraction of UD-Cs, T-C and 0/90-C.

The initial flexural properties of textile reinforced composites, 0 ⁄90 ° lay-up composite and neat PLA plate are presented in

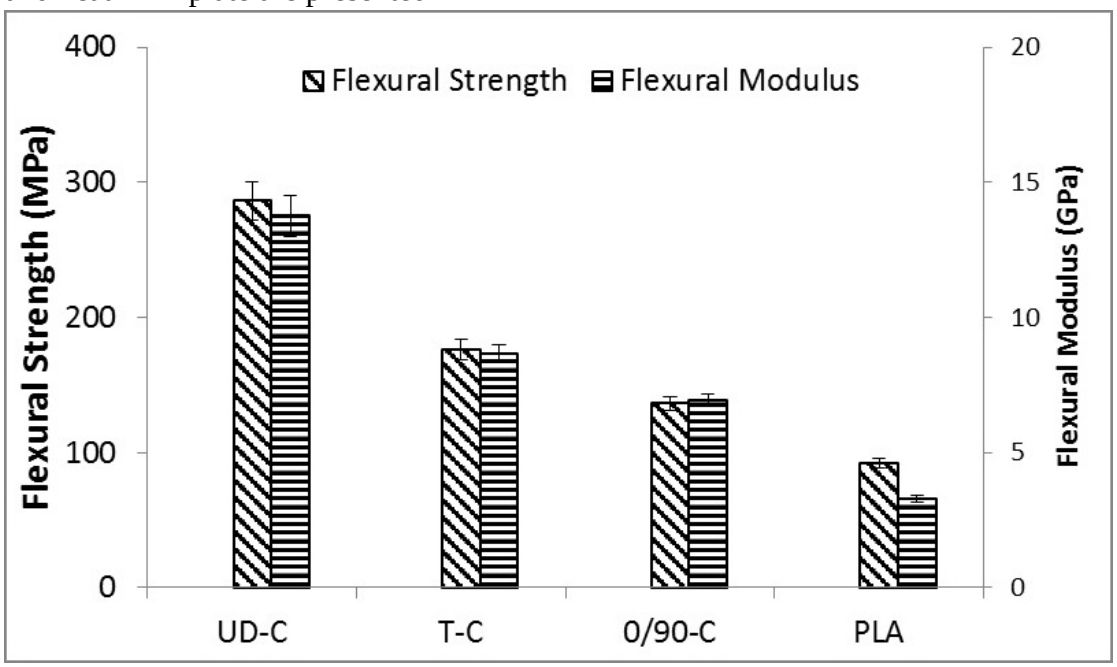

Figure *4*, where it can be seen that the flexural strength and modulus of neat PLA plate improved as expected due to reinforcement with textile and unidirectional fiber mats. Additionally, with the similar fiber volume fraction (~20%), the flexural strength of neat PLA plate was seen to increase from 92 ± 6 MPa to 286 ± 14 MPa for the UD-C, to 176 ±13 MPa for the T-C and to 137 ± 9 MPa for the 0/90-C. Addition of the reinforcement phases improved the flexural modulus of neat PLA from 3.3 ± 0.1 GPa to 13.8 ± 0.7 GPa, 8.6 ± 0.3 GPa and 6.9 ± 0.2 GPa for the UD-C, T-C and 0/90-C, respectively. As such, the textile reinforced composite exhibited statistically significantly higher ($P<0.01$) flexural strength and modulus when compared to those of the 0/90-C and neat PLA plate, whilst the highest flexural strength and modulus was observed for the UD-C.

Degradation study of composites

The degradation of textile reinforced composites (T-C), 0 ⁄90 ° lay-up composite (0/90-C), UD fiber mat reinforced composite (UD-C) and neat PLA plate was investigated in PBS at 37 ℃ for up to 28 days. As can be seen from

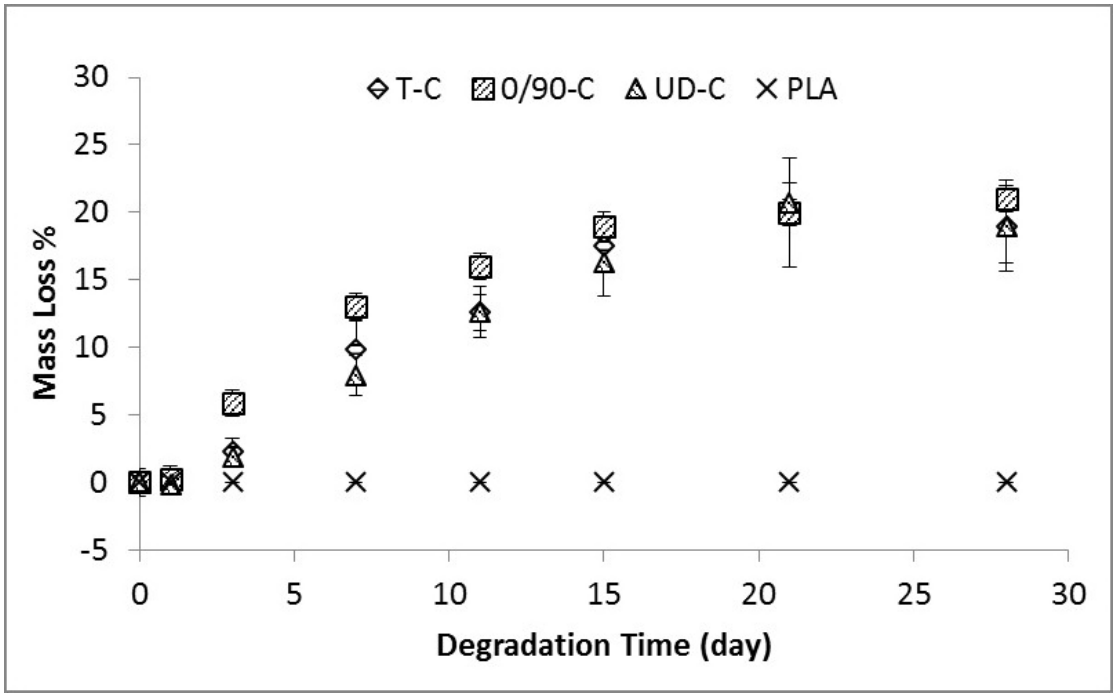

Figure 5, a significantly higher mass loss was observed for the 0/90-C during the first 11 days. However, by 21 days the mass loss had converged for all the composite samples. All the composites demonstrated a much higher mass loss when compared to neat PLA. The composites all lost ~20% mass by 28 days, while the neat PLA plate had a mass loss of only ~0.05% during the 28 day study.

Water uptake throughout the 28 day study is shown in

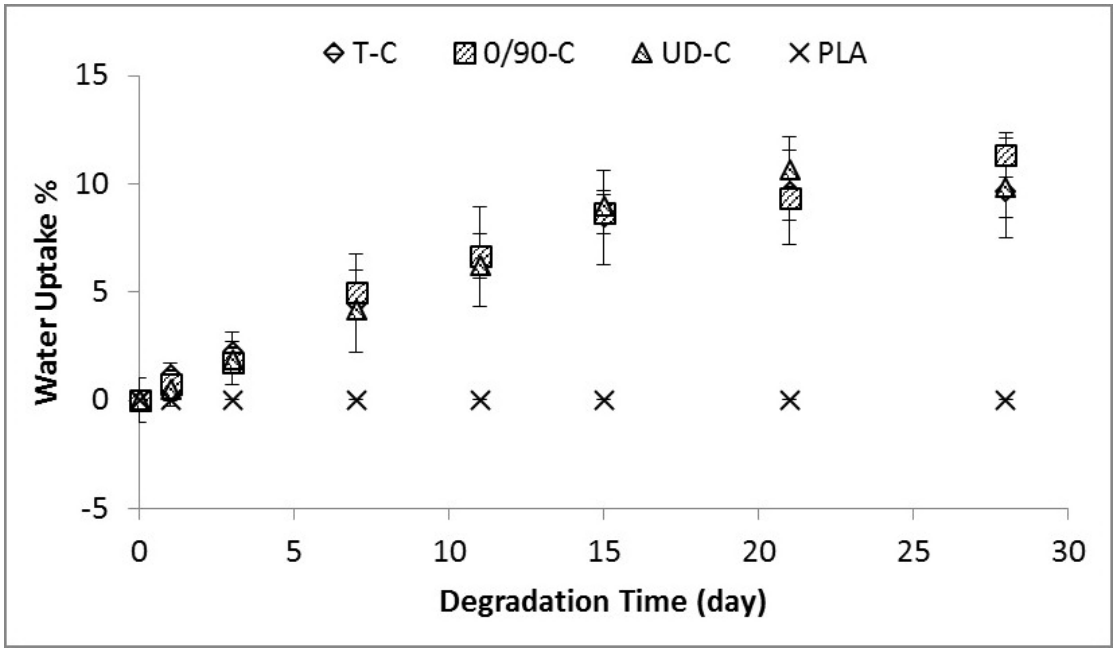

Figure 6. The water uptake of all the composites was seen to increase over the duration of the study. After 28 days of immersion in PBS at 37 ℃, the water uptake of the T-C and 0/90-C reached ~10 wt%, and no significant difference ($P>0.05$) in the value of water uptake was found when compared to the UD-C. However, the pure PLA plate did not exhibit much water uptake with a value of 0.84 wt%.

The pH of the PBS solution during the degradation study period was measured and fresh PBS was replaced at each time point. As can be seem from

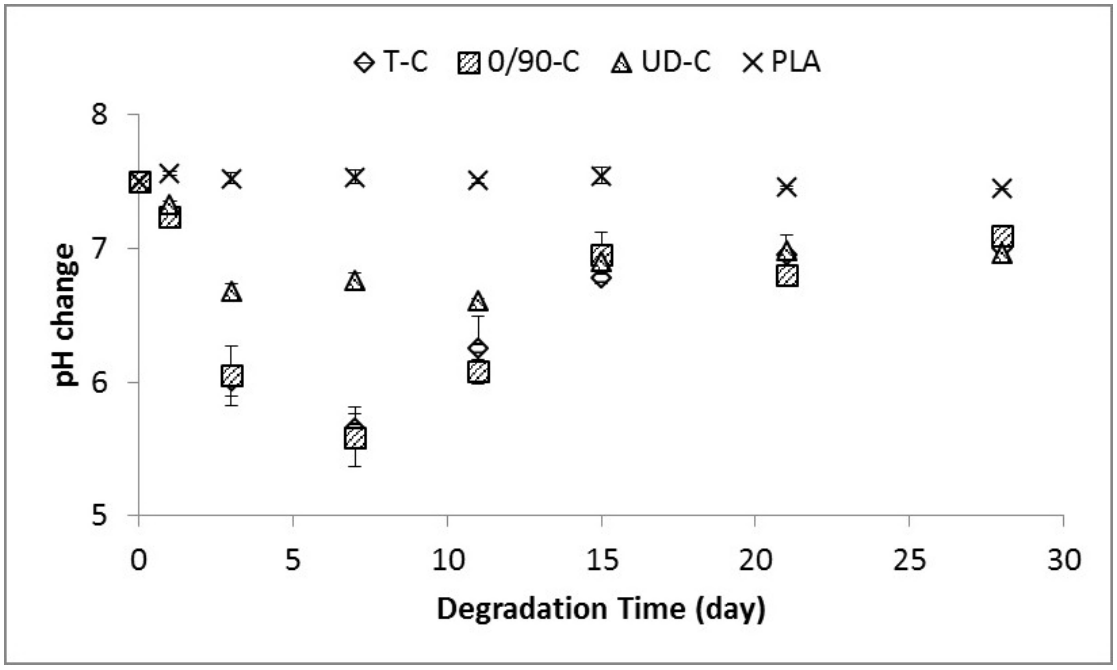

Figure 7, the pH decrease was higher for the textile reinforced composites (T-C) and 0 ⁄90 ° lay-up composites (0/90-C), falling to a minimum of 5.5 after 7 days. The pH for the UD-C also decreased significantly, to 6.5. The pH value of all the composites fluctuated and reached a relatively stable status after 21 days of degradation. The pH value of neat PLA remained relatively neutral over the duration of the study.

Crystallinity

The change in crystallinity of the PLA matrix polymer was determined using DSC (see

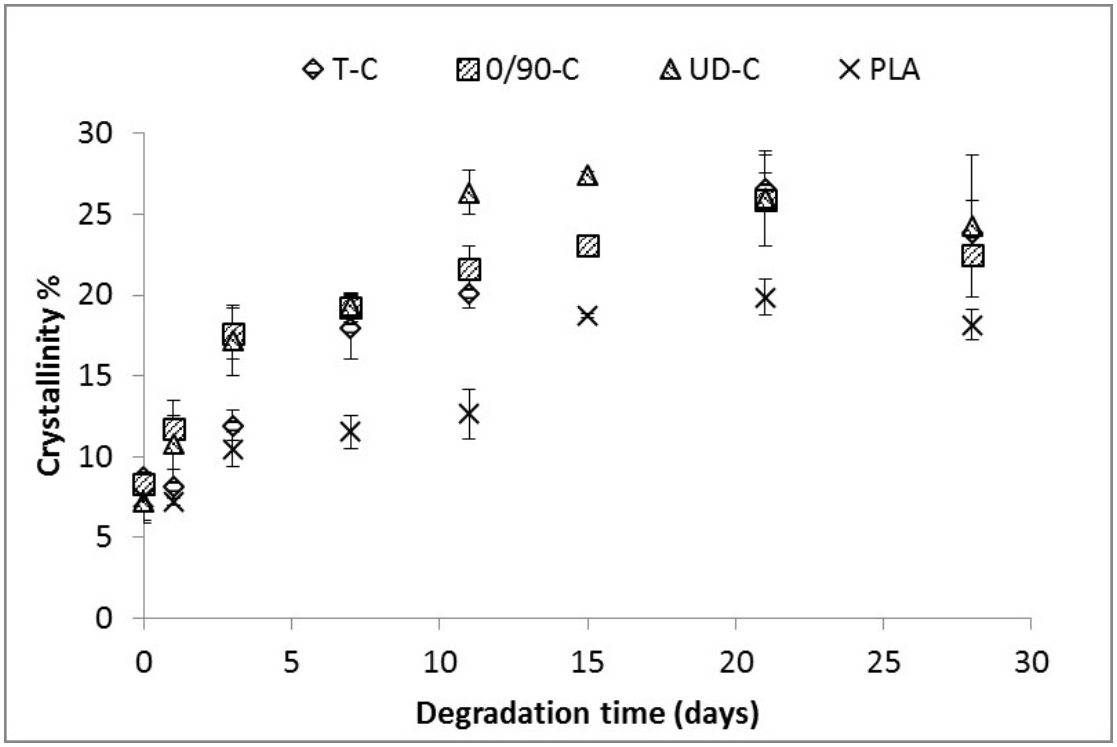

Figure 8). It was observed that the crystallinity of the PLA increased significantly with addition of the reinforcement phase. For neat PLA, crystallinity increased from ~7% to ~18% over the course of the 28 days degradation study. However, the crystallinity of the PLA matrix in of all composites (T-C, 0/90-C and UD-C) increased more rapidly than the neat PLA, reaching ~24% after immersion for 28 days in PBS. Moreover, in comparison with T-C and 0/90-C, crystallinity of UD-C increased and peaked by day 11.

Retention of the flexural properties

The flexural strength and modulus of the Textile-composite, 0/90-C, UD-C and neat PLA plate were plotted against degradation time in

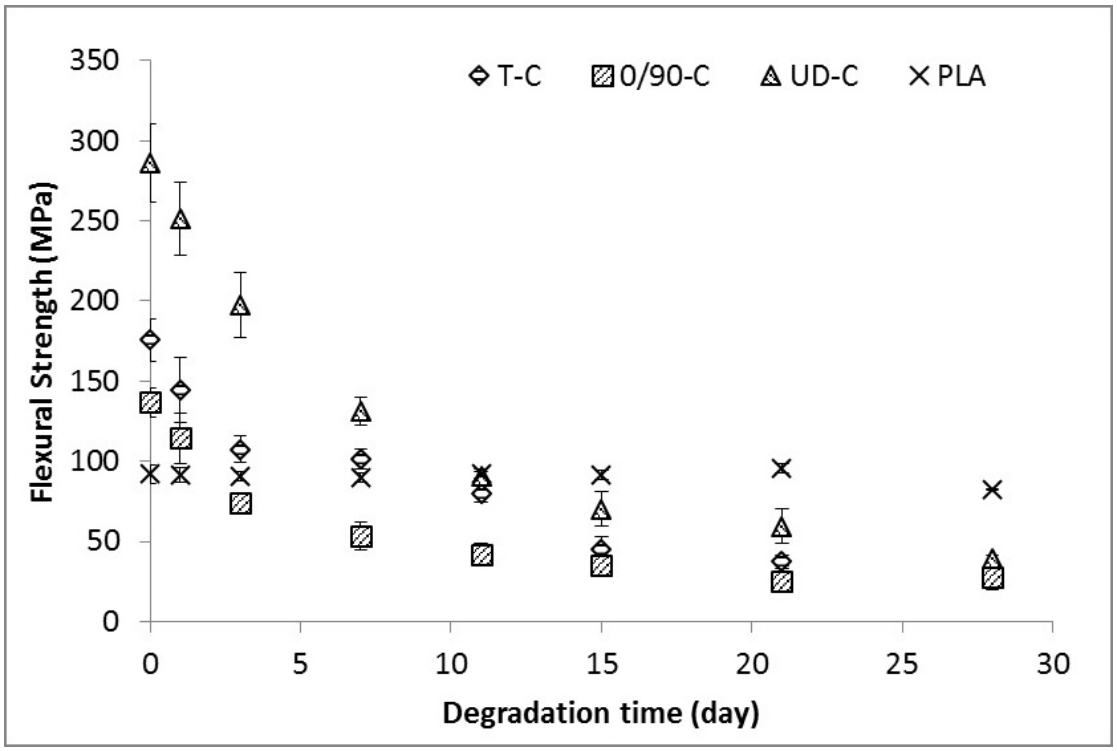

Figure 9 and

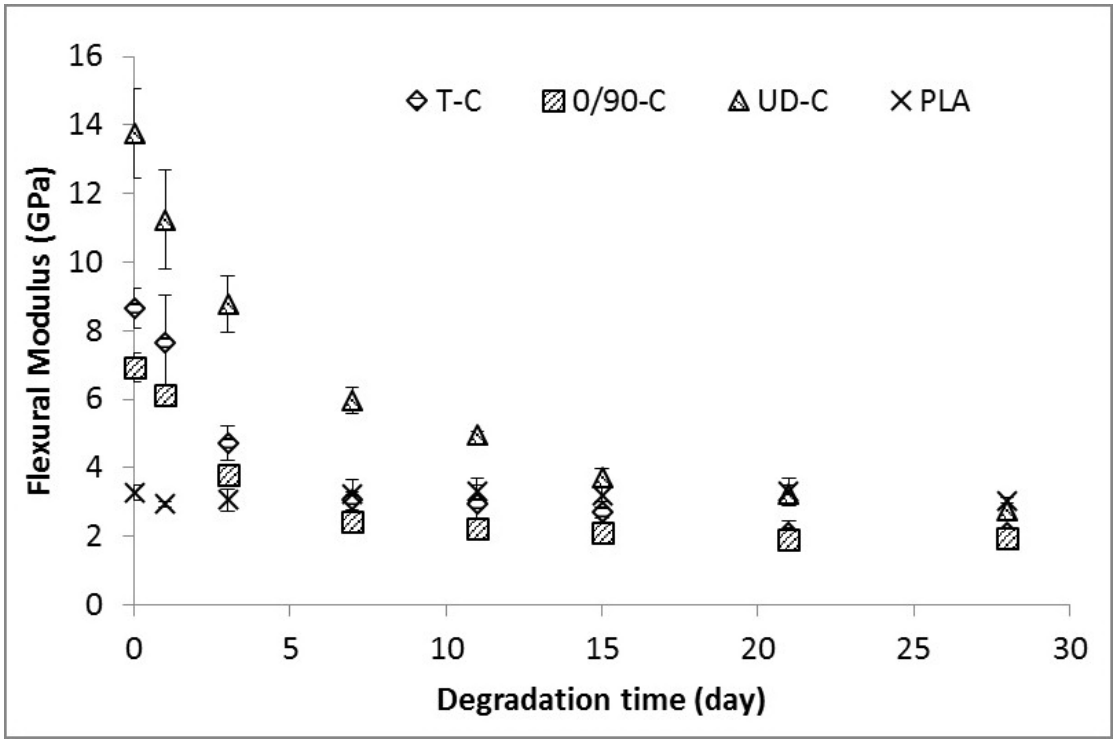

Figure 10, respectively. The UD-Cs were seen to achieve significantly higher ($P<0.01$) initial flexural strength, as compared to the initial flexural strength values for the other composites and the neat PLA plate. The flexural strength of the T-C and 0/90-C revealed a rapid decrease within the first 7 days of the degradation period, falling from 176 ± 13 MPa and 137 ± 9 MPa to 108 ± 8 MPa and 74 ± 5 MPa respectively. They reached final values of 32 ± 3 MPa and 28 ± 8 MPa after 28 days. The UD-C demonstrated a rapid decrease in flexural strength from 286 ± 25 MPa to 91 ± 3 MPa over the course of the initial 11 days of immersion in PBS. No significant ($P>0.05$) difference in flexural strength was observed between the three composites at day 28. No significant change in the flexural strength was observed for neat PLA during the course of the study.

The non-degraded Textile-composite, 0/90-C and UD-C achieved initial flexural modulus values of 9 ± 1 GPa, 7 ± 1 GPa and 14 ± 1 GPa, respectively. The flexural modulus of the

composites reinforced by textile and by 0 ⁄90 ° lay-up UD fiber mats showed the same trend after immersion in PBS, with a decrease seen at day 7 and a further slight decrease by day 28. However, the UD-C revealed a more gradual decline in flexural modulus over the first 11 days.

The flexural modulus for the T-C and the 0/90-C reduced to ~3 GPa after 7 days and plateaued at ~2 GPa after 28 days of immersion in PBS. The UD-C presented a similar value of flexural modulus after 15 days of degradation and remained relatively constant at ~3 GPa up to day 28. The modulus of the neat PLA remained relatively constant at ~3 GPa throughout the 28 day degradation period.

SEM analysis

Images of the fracture surfaces of the composites taken during the degradation study are presented in

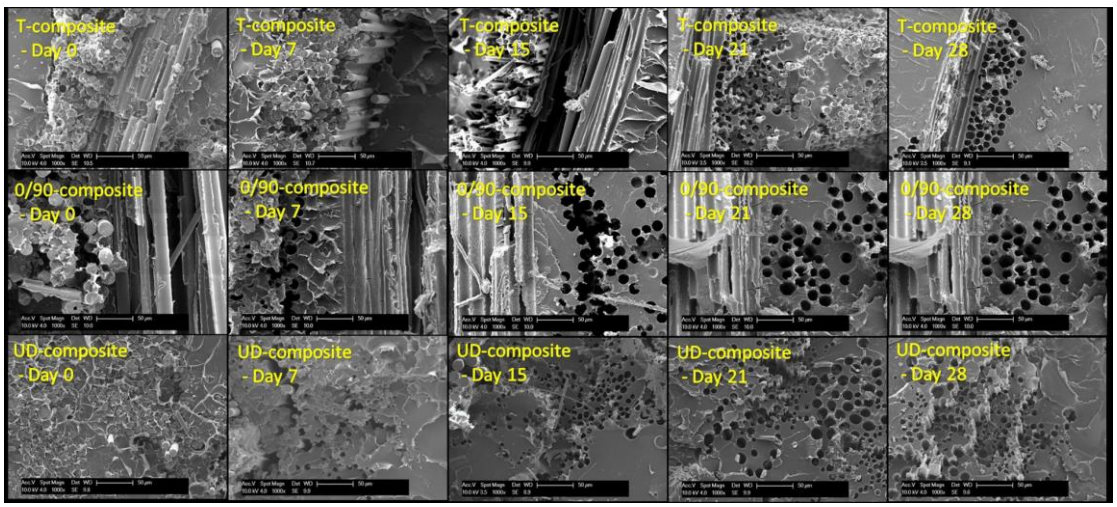

Figure 11. Overall, debonding between fiber and PLA matrix was seen for all the composites after 7 days of immersion in PBS. Due to the apparent degradation of fiber

and fiber pull-out during the three point bending tests, pores and channels were observed in all composites. Furthermore, no fiber was seen in the images of the 0/90-C after 15 days of degradation, and T-C after 28 days degradation.

Discussion

This study manufactured yarns and textiles from phosphate glass fibers. The yarns were twisted and coated with water soluble epoxy resin, which provided additional integrity and surface protection, making them more suitable (i.e. easier to handle) for the weaving process. Therefore, only yarns with twist were used in the textile manufacturing process. Industrial weaving equipment has been designed for E-glass and S-glass fiber, which have relatively higher tensile strength values (quoted as ~3000 MPa [52, 58]) in comparison to that of the phosphate glass fibers used in this study (~1000 MPa). At present, the industrial weaving process of phosphate glass fibers is still under development in order to make adjustments to allow for this lower strength. As such, hand weaving via use of a small Inkle-type loom was utilized as a short-term solution to weave lab scale textiles for testing [46, 59].

The composites in this study were reinforced using 20% V_f of textile fabric (T-C) or unidirectional fiber mats (UD-C and 0/90-C) of the glass system $48P_2O_5$-$12B_2O_3$-$14CaO$-$20MgO$-$1Na_2O$-$5Fe_2O_3$. The flexural properties of the UD-C were presented for comparison. The burn off test confirmed that there was no significant ($P>0.05$)

difference in fiber volume fraction between the UD-C, T-C and 0/90-C. As shown in

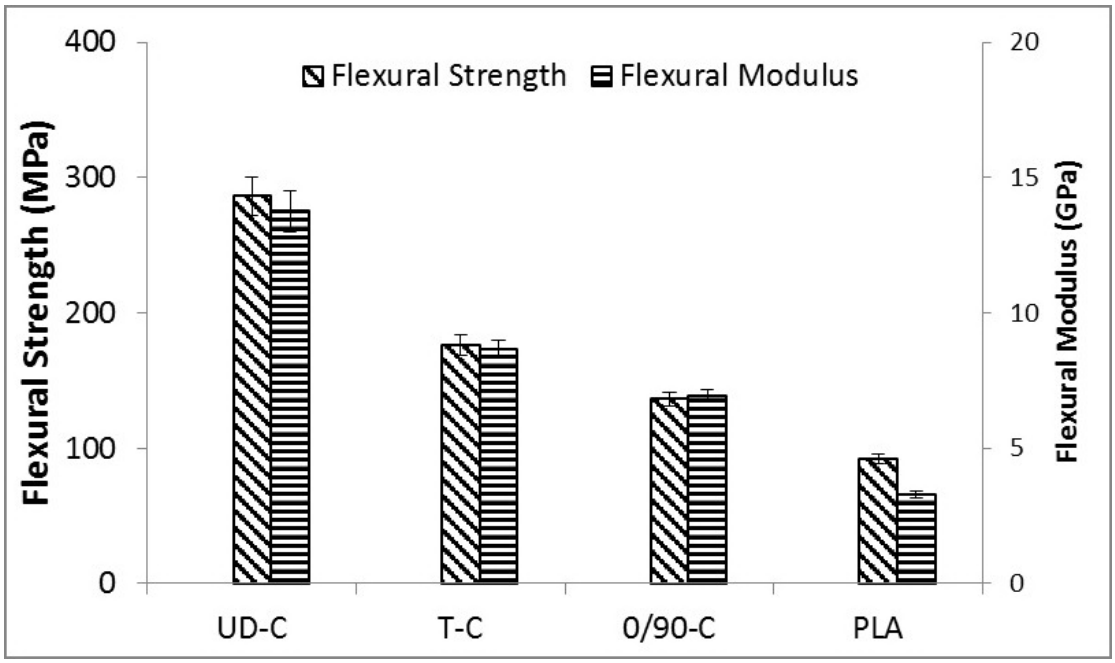

Figure *4*, the dry flexural strength and modulus values for the Textile-composite (T-C) were 29% and 25% higher than those of the 0/90-C, respectively. However, the UD-C presented significantly higher flexural strength and modulus when compared to the T-C and 0/90-C in this study.

The 0/90-C was manufactured via laminate stacking UD fiber mats in 0 ⁰/90 °directions and the fiber fractions in the longitudinal and transverse directions were similar at 50%. Ordinarily, a plain weave textile would be balanced and have 50% of yarns in the warp direction and 50% in the weft direction. This type of fabric has a number of interlacing points (where the weft thread passes over the warp thread and then under the next warp in turn), so that the final fabric is stronger than other weave types such as twill weave for example [60, 61]. However, due to limitations with the hand weaving process, it was difficult to maintain an equivalent density of the warp and weft yarns. As can be seen from Table 1, for a single laminate of textile fabric there were considerably more yarns (~79%) along the longitudinal (warp) direction than in the in transverse (weft) direction (~21%). Nassif [62] reported that the increase in density of yarns parallel to

the load direction lead to an increase in textile fabric stiffness due to the increase in yarn quantity and improvement of load capacity. Therefore, the composite with higher density of warp parallel to the load (longitudinal) direction demonstrated greater mechanical properties. It was also the reason why the UD-C with entirely unidirectional fibers along the longitudinal direction showed higher mechanical properties than the textile or 0 ⁄90 ° fiber mat reinforced composites.

In order to compare the mechanical properties of a composite which has a varying proportion of fibers along the warp direction, a rule of mixtures approach (ignoring crimp) was used. This is shown in

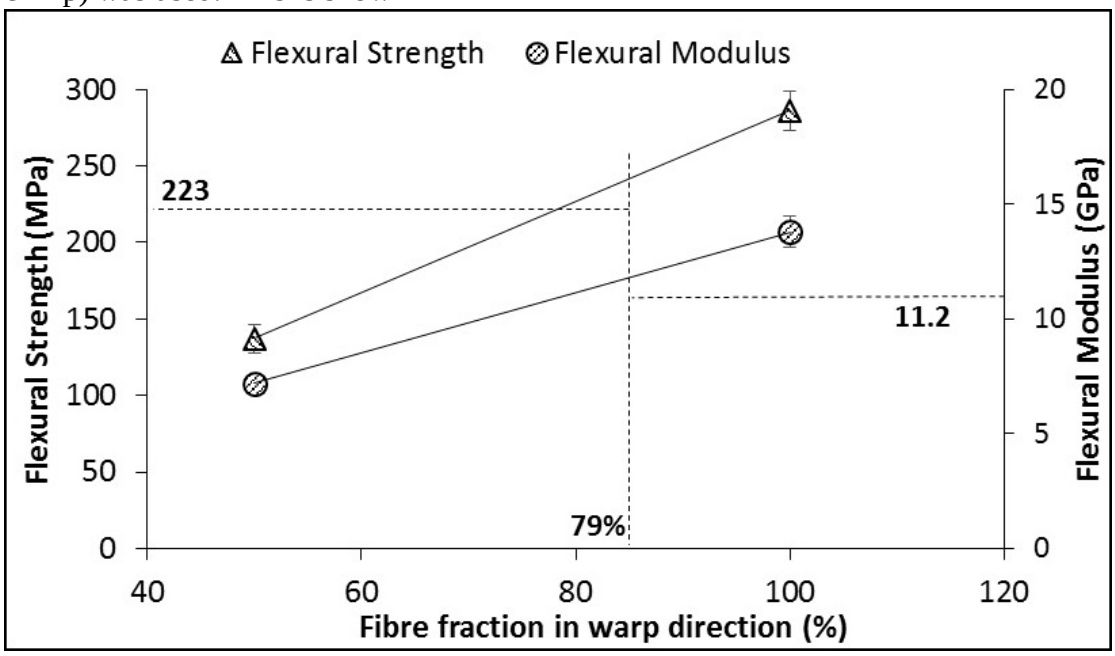

Figure *12*, with the flexural properties of a composite with 79% of fibers in the warp direction calculated as having a flexural strength of 223 MPa and a flexural modulus of 11.2 GPa. These values were significantly higher than the experimental results achieved for the T-C composite. This could be accounted for by considering the effect of the textile crimp, which can cause high stress concentrations in the crimped region [63]. Yang et al. [64] reported that plain weave glass fiber reinforced composites presented 15% lower compressive strength when compared to composites reinforced by non-crimp laminate glass fiber mats. Utilizing this 15% decrease in properties as suggested,

the expected strength of the T-C composite would be approximately 190 MPa, which was much closer to what was observed experimentally.

All the composites saw a continuous mass loss during the degradation study and there was no significant difference between them over the 28 day duration of the study. However, the degradation behavior indicated a higher mass loss for the 0/90-C during the initial 15 days degradation period when compared to the other composites. The primary factors affecting the degradation were degradation of bonding between fibers and matrix resin due to hydrolysis of coupling agent on the surfaces of fibers, and weakening of the strength of glass fibers due to the fiber dissolution [65]. Since the mass loss of the neat PLA plate appeared to be negligible, the mass loss of the composite was attributed to the dissolution of phosphate glass fiber. The UD-Cs were open-ended, which meant that the fiber ends were exposed at the edges of the composites. This could allow water to wick along the fiber/matrix, causing the fibers to degrade from two ends to the middle region.

The mass loss profiles and the pH changes suggest that the degradation of the 0/90-C was more rapid than for the UD-C and T-C. The degradation mechanism diagram in

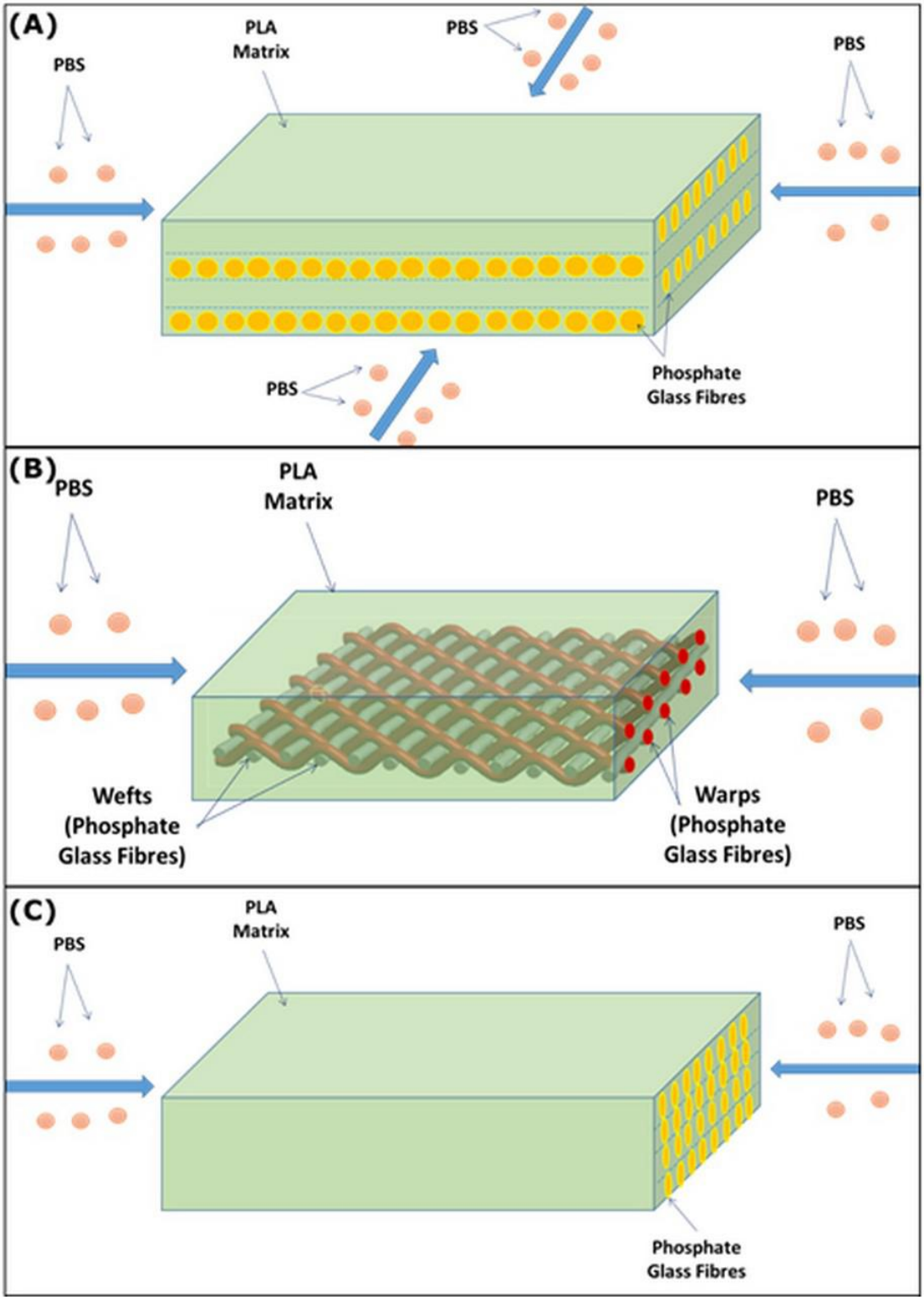

Figure *13* indicated that PBS was able to attack all edges of 0/90-C and dissolve the fibers along the longitudinal and transverse directions. However, only two ends of T-C and UD-C in longitudinal direction allowed water ingress as well as UD-C.

Additionally, T-C presented more yarns lying in the longitudinal direction when compared to 0/90-C, providing a longer overall path length for the water to ingress which possibly could have delayed or inhibited the degradation process.

The increase in crystallinity of PLA was attributed to three primary factors: (1) degradation of the amorphous part of the polymer leaving the more hydrolysis resistant crystalline phase [66]; (2) the hydrolysis of ester bonds in the amorphous phase of the polymer resulting in shorter polymer chains that can crystallize more easily [67, 68]; (3) the plasticization effect of water which resulted in an increase of the mobility of polymer chains [57, 69].

It was seen that the crystallinity of neat PLA and the PLA matrix of the composites increased during immersion in PBS over 28 days. However, as no significant difference ($P>0.05$) in crystallinity of the PLA matrix was observed amongst the UD-C, T-C and 0/90-C by 28 days in this study, the crystallinity of PLA was considered to be independent on reinforcement type of the composites. On the other hand, matrix PLA of all the composite samples showed a higher degree of crystallinity than neat PLA. It was explained by Arroyo et al. [70] who investigated the crystallization kinetics of polymer composites with various glass fiber volume fractions, and suggested that the crystallinity was higher in the composites due to the nucleating effect of the fires in the composite [70]. Manchado et al. [71] also provided evidence of spherulite growth with the transcrystallinity on the surface of the polymer bonding to fibers and confirmed the fiber in composites behaved as effective nucleation agents for the crystallization of polymer matrix.

A rapid reduction in flexural strength and modulus was observed for UD-C, T-C and 0/90-C during the first 7 days of degradation period, whilst all composites presented a

relatively smooth decrease in flexural properties until day 28. Moreover, a relatively higher flexural strength and modulus was observed for T-Cs when compared to 0/90-C during the initial 15 days degradation period. However, no significant difference was observed for flexural properties of both composites after 28 days of immersion in PBS. Over the period of immersion in PBS, T-C and 0/90-C revealed 82% and 80% reduction in flexural strength respectively, whilst the flexural modulus of both composites had decreased by 76% and 72% respectively.

In comparison with the mass loss of all composites in

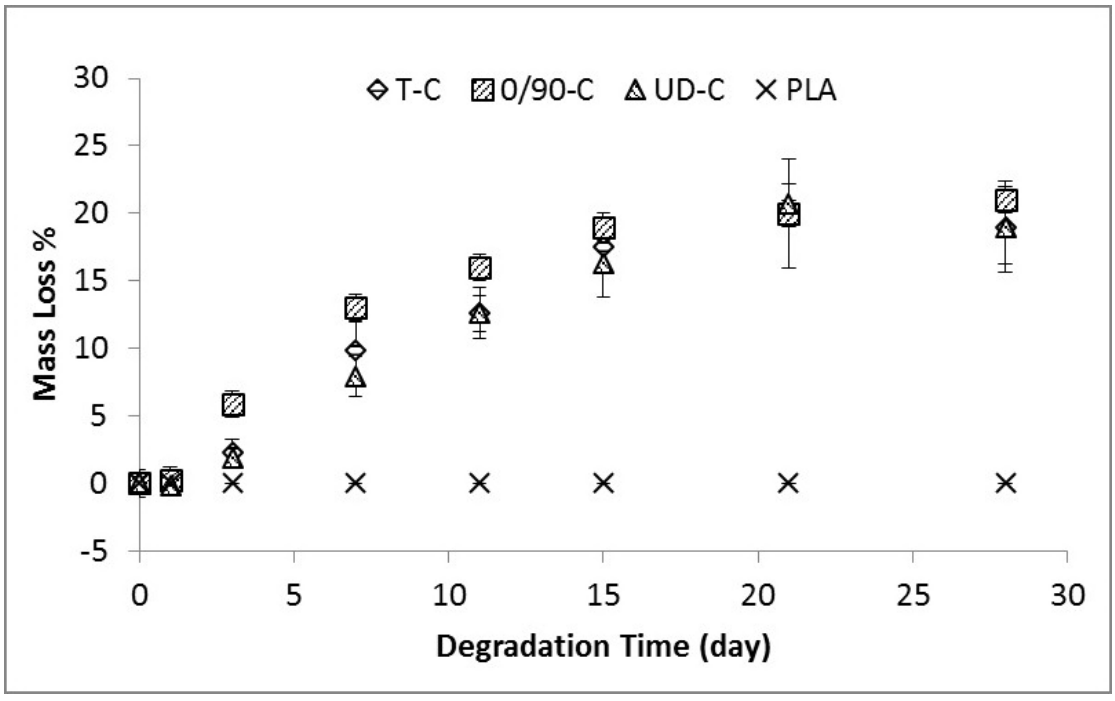

Figure 5, it was evident that the retention of mechanical properties was associated with fiber dissolution. Hull [72] and Gibson [73] explained that the mechanical properties of composites were dependent on the fibers and polymer matrix for load bearing and the interfacial bonding between fiber and matrix for load transfer. The flexural strength and modulus decrease with time was due to the water which diffused into composite samples, acting as a plasticizer and reducing the mechanical properties of the PLA matrix [38]. Additionally, water that diffused into the composite samples was able to

degrade the interface between fiber and matrix, resulting in poor stress transfer efficiency and reduction of flexural properties [74, 75]. This phenomenon is referred to as the “wicking effect” and has been investigated by several researchers [76, 77] who stated that it was a form of capillary action between the fibers and matrix resulting in loss of the reinforcing effect. This explanation was supported by microscopy images of composites in

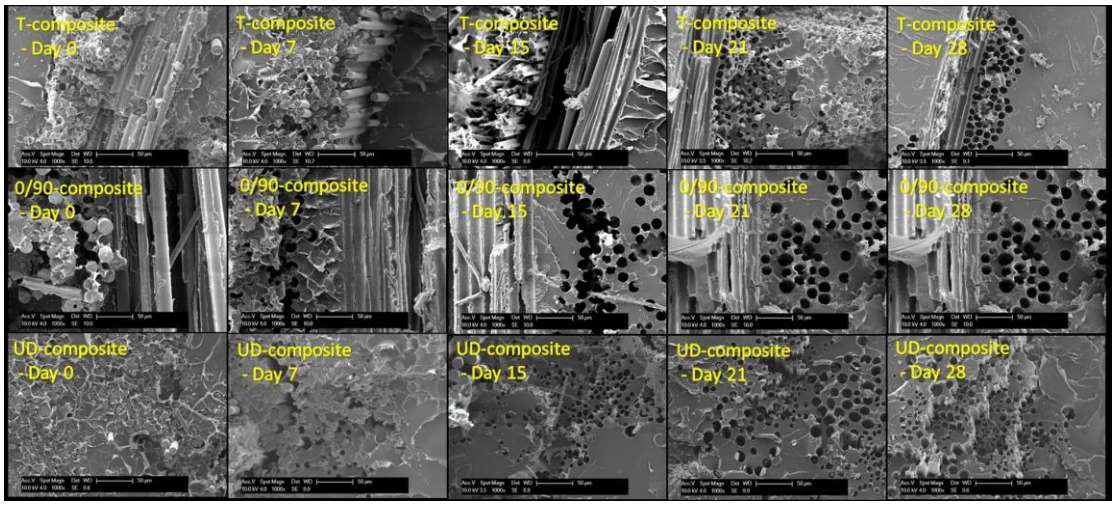

Figure 11, the interface of T-C and 0/90-C was degraded and short fiber pull-out was observed after 7 days of degradation study.

In this study, phosphate glass fiber textiles were produced and utilized as composite reinforcement. Initially, this novel composite was a good preliminary study to investigate feasibility of industrial scale production of phosphate glass fiber reinforced composites. However, the results in this paper revealed some important challenges. For example, the degradation study of the composites revealed that the phosphate glass fiber degraded too fast, resulting in a significant reduction of mechanical properties of composite due to dissolution of fiber and fiber-matrix interface. As such, the development of suitable coating agent to protect the fiber surface and improve fiber-matrix interface via forming chemical bonding should be taken into account for follow-

on studies. Further, there were limitations in the textile hand weaving process such as low weaving efficiency, different warp and weft density and difficulty in controlling crimps of textile. Automation of the textile manufacturing process via a suitable weaving machine (suitable for PGFs) should be investigated further in order to produce uniform textile fabrics. In a word, this achievement will be the significant milestone on the research of bioresorbable PGFs reinforced composite in medical application, and important step on the industrial direction of bioresorbable medical device.

Conclusions

This research reported on the first PGF textile products developed for composite reinforcement using yarns produced through industrial processes. Multifilament yarns produced from $48P_2O_5$-$12B_2O_3$-14CaO-20MgO-$1Na_2O$-$5Fe_2O_3$ were successfully converted into woven textiles using an Inkle loom. The results indicated that the textile

reinforced composite performed with comparable efficacy to the composite reinforced by UD fiber mats, when accounting for fabric bias and degree of crimp. However, the degradation rate of all of the composites was faster than desired, with only ~20% flexural strength and ~25% flexural modulus maintained by the 28 day time point. A suitable coating agent and automatic weaving technique should be investigated in further study.

Acknowledgements

This research did not receive any specific grant from funding agencies in the public, commercial, or not-for-profit sectors. However, the authors would like to acknowledge the financial support from Ningbo 3315 Innovation team Scheme “Composites Development and Manufacturing for Sustainable Environment”. They also appreciate

the support received from Sinoma Co.,Ltd (China) for their assistance in developing the technology to produce phosphate glass fiber textiles.

Reference

1. J. Malekani, B. Schmutz, Y. Gu, M. Schuetz, and P.K. Yarlagadda. *Biomaterials in orthopedic bone plates: a review*. *The 2nd Annual International Conference on Materials Science, Metal & Manufacturing*. (2011)
2. M. Navarro, A. Michiardi, O. Castano, and J. Planell, *J Roy Soc Interface*. **5**, 1137-1158 (2008)
3. B.D. Ratner, A.S. Hoffman, F.J. Schoen, and J.E. Lemons, *Biomaterials science: an introduction to materials in medicine*, 2014, ACADEMIC PRESS 484 (2014)
4. Q. Fu, E. Saiz, M.N. Rahaman, and A.P. Tomsia, *Mater Sci Eng C Mater* **31**, 1245-1256 (2011)

5. S. Yu, Z. Yu, G. Wang, J. Han, X. Ma, and M.S. Dargusch, *Colloid Surface B.* **85**, 103-15 (2011)
6. Z. Huang, *Compos Sci Technol*. **65**, 73-85 (2005)
7. I. Ahmed, I. Jones, A. Parsons, J. Bernard, J. Farmer, C. Scotchford, G. Walker, and C. Rudd, *J Mater Sci: Mater M*. **22**, 1825-1834 (2011)
8. A. Tonino, C. Davidson, P. Klopper, and L. Linclau, *J Bone Joint Surg Br*. **58**, 107-113 (1976)
9. H. Schwyzer, J. Cordey, S. Brun, P. Matter, and S. Perren, *Bone loss after internal fixation using plates, determination in humans using computed tomography*, 1985, Springer 191-195 (1985)
10. J. Wolff, *Das Gesetz der Transformation der inneren Architektur der Knochen bei pathologischen Veränderungen der äusseren Knochenform*, 1884, Gedruckt in der Reichsdruckerei (1884)
11. M. Bitar, V. Salih, V. Mudera, J.C. Knowles, and M.P. Lewis, *Biomaterials*. **25**, 2283-2292 (2004)
12. A.J. Parsons, I. Ahmed, N. Han, R. Felfel, and C.D. Rudd, *J Bionic Eng*. **7**, S1-S10 (2010)
13. R.L. Prabhakar, S. Brocchini, and J.C. Knowles, *Biomaterials*. **26**, 2209-18 (2005)
14. R.A. Khan, A.J. Parsons, I.A. Jones, G.S. Walker, and C.D. Rudd, *J Reinf Plast Comp*. **29**, 1838-1850 (2009)
15. J. Tams, F.R. Rozema, R.R.M. Bos, J.L.N. Roodenburg, P.G.J. Nikkels, and A. Vermey, *Int J Oral Max Surg*. **25**, 20-24 (1996)
16. S. Ramakrishna, J. Mayer, E. Wintermantel, and K.W. Leong, *Compos Sci Technol*. **61**, 1189-1224 (2001)
17. D. Brauer, C. Rüssel, S. Vogt, J. Weisser, and M. Schnabelrauch, *J Mater Sci: Mater M*. **19**, 121-127 (2008)
18. K. Fujihara, *Biomaterials*. **24**, 2661-2667 (2003)
19. K. Fujihara, Z.M. Huang, S. Ramakrishna, K. Satknanantham, and H. Hamada, *Biomaterials*. **25**, 3877-85 (2004)
20. M.S. Mohammadi, I. Ahmed, N. Muja, S. Almeida, C.D. Rudd, M.N. Bureau, and S.N. Nazhat, *Acta Biomater*. **8**, 1616-26 (2012)
21. L.L. Hench, and H. Paschall, *J Biomed Mater Res A*. **7**, 25-42 (1973)
22. L.L. Hench, R.J. Splinter, W.C. Allen, and T.K. Greenlee, *J Biomed Mater Res A*. **5**, 117-141 (1971)
23. L. Hench, *J Mater Sci: Mater M*. **17**, 967-978 (2006)
24. G. Furtos, M. Tomoaia-Cotisel, B. Baldea, and C. Prejmerean, *J Appl Polym Sci*. **128**, 1266-1273 (2013)
25. G. Furtos, M. Tomoaia-Cotisel, and C. Prejmerean, *Particul Sci Technol*. **31**, 332-339 (2013)
26. M.N. Rahaman, D.E. Day, B.S. Bal, Q. Fu, S.B. Jung, L.F. Bonewald, and A.P. Tomsia, *Acta Biomater*. **7**, 2355-73 (2011)
27. I. Ahmed, E.A. Abou Neel, S.P. Valappil, S.N. Nazhat, D.M. Pickup, D. Carta, D.L. Carroll, R.J. Newport, M.E. Smith, and J.C. Knowles, *J Mater Sci*. **42**, 9827-9835 (2007)
28. C. Zhu, I. Ahmed, A. Parsons, K.Z. Hossain, C. Rudd, J. Liu, and X. Liu, *J Non-Cryst Solids*. **457**, 77-85 (2017)
29. J.C. Knowles, *J Mater Chem*. **13**, 2395-2401 (2003)
30. C. Tan, I. Ahmed, A.J. Parsons, N. Sharmin, C. Zhu, J. Liu, C.D. Rudd, and X. Liu, *J Mater Sci*. 1-14 (2017)

31. W. Liang, M.N. Rahaman, D.E. Day, N.W. Marion, G.C. Riley, and J.J. Mao, *J Non-Cryst Solids*. **354**, 1690-1696 (2008)
32. R.F. Brown, M.N. Rahaman, A.B. Dwilewicz, W. Huang, D.E. Day, Y. Li, and B.S. Bal, *J Biomed Mater Res A*. **88**, 392-400 (2009)
33. L. Balachander, G. Ramadevudu, M. Shareefuddin, R. Sayanna, and Y.C. Venudhar, *ScienceAsia*. **39**, 278 (2013)
34. I. Ahmed, M. Lewis, I. Olsen, and J.C. Knowles, *Biomaterials*. **25**, 491-499 (2004)
35. J. Choueka, J.L. Charvet, H. Alexander, Y.H. Oh, G. Joseph, N.C. Blumenthal, and W.C. LaCourse, *J Biomed Mater Res A*. **29**, 1309-1315 (1995)
36. I. Ahmed, M. Lewis, I. Olsen, and J.C. Knowles, *Biomaterials*. **25**, 501-507 (2004)
37. I. Ahmed, P.S. Cronin, E.A. Abou Neel, A.J. Parsons, J.C. Knowles, and C.D. Rudd, *J Biomed Mater Res B*. **89**, 18-27 (2009)
38. R.M. Felfel, I. Ahmed, A.J. Parsons, P. Haque, G.S. Walker, and C.D. Rudd, *J Biomater Appl*. **26**, 765-89 (2012)
39. N. Sharmin, A.J. Parsons, C.D. Rudd, and I. Ahmed, *J Biomater Appl*. **0**, 1-15 (2014)
40. N. Sharmin, M.S. Hasan, A.J. Parsons, D. Furniss, C.A. Scotchford, I. Ahmed, and C.D. Rudd, *Biomed Res Int*. **2013**, 1-12 (2013)
41. N. Sharmin, M.S. Hasan, A.J. Parsons, C.D. Rudd, and I. Ahmed, *J Mech Behav Biomed Mater*. **59**, 41-56 (2016)
42. I. Ahmed, A. Parsons, J. Liu, and C.D. Rudd. *Phosphate-based glass fibres: applications within heathcare*. *International Glass Fiber Symposia* (2012)
43. D.S. Brauer, C. Russel, W. Li, and S. Habelitz, *J Biomed Mater Res A*. **77**, 213-9 (2006)
44. E.A. Abou Neel, I. Ahmed, J.J. Blaker, A. Bismarck, A.R. Boccaccini, M.P. Lewis, S.N. Nazhat, and J.C. Knowles, *Acta Biomater*. **1**, 553-63 (2005)
45. E.A. Abou Neel, A.M. Young, S.N. Nazhat, and J.C. Knowles, *Adv Mater*. **19**, 2856-2862 (2007)
46. A.C. Long, *Design and manufacture of textile composites*, 2006, Taylor & Francis (2006)
47. J. Liu, Q. Zu, C. Rudd, S. Huang, and X. Liu, CN 201610188354, 2016
48. L. Chen, Y. Gu, Y. Feng, X.S. Zhu, C.Z. Wang, H.L. Liu, H.Y. Niu, C. Zhang, and H.L. Yang, *J Mater Sci: Mater M*. (2014)
49. Y. Wang, X. Liu, C. Zhu, A. Parsons, J. Liu, I. Ahmed, and C. Rudd. *Novel phosphate glass fibre textile composites for implants*. *SAMPE China 2016 Conference and exhibition*. (2016)
50. Y. Wang, N. Sharmin, A. Parsons, X. Liu, J. Liu, I. Ahmed, and C. Rudd. *Novel bioresorbable textile composite for biomedical applications*. *The 5th International Conference of Boimic Engineering*. (2016)
51. K.L. Loewenstein, *Manufacturing Technology of Continuous Glass Fibres*, 1973, Elsevier Science Ltd 296 (1973)
52. F.T. Wallenberger, J.C. Watson, and H. Li, *Glass fibers*, 21, 2001, ASM International 27-34 (2001)
53. ASTM D2584-11: 2011, Standard Test Method for Ignition Loss of Cured Reinforced Resins.
54. BS 10993-13:2010, Biological evaluation of medical devices: Part 13.

55. BS 14125: 1998, Fibre-reinforced plastic composites - Determination of flexural properties.
56. M.R. Kessler, *Advanced topics in characterization of composites*, 2004, Trafford Publishing (2004)
57. R.A. Auras, L.T. Lim, S.E.M. Selke, and H. Tsuji, *Poly(lactic acid): synthesis, structures, properties, processing, and applications*, 2011, Wiley (2011)
58. D.R. Messier, and P.J. Patel, *J Non-Cryst Solids*. **182**, 271-277 (1995)
59. N. Gokarneshan, *Fabric structure and design*, 2004, New Age International (P) Ltd. (2004)
60. M.A. Taylor, *Technology of textile properties: an introduction*, 1981, Forbes Publications Ltd (1981)
61. W. Zhong, *An Introduction to Healthcare and Medical Textiles*, 2013, DEStech Publications (2013)
62. G.A.A. Nassif, *Life Sci J*. **8**, (2012)
63. S. Kari, M. Kumar, I. Jones, N. Warrior, and A. Long. *Effect of yarn cross-sectional shapes and crimp on the mechanical properties of 3D woven composites*. *The 17th International Conference on Composite Materials*. (2008)
64. B. Yang, V. Kozey, S. Adanur, and S. Kumar, *Compos Part B: Eng*. **31**, 715-721 (2000)
65. H. Sekine, K. Shimomura, and N. Hamana, *JSME Int J I-Solid M*. **31**, 619-626 (1988)
66. N. Sultana, and T.H. Khan, *J Nanomater*. **2012**, 1 (2012)
67. S. Li, H. Garreau, and M. Vert, *J Mater Sci: Mater M*. **1**, 123-130 (1990)
68. Z. Zhou, Q. Yi, L. Liu, X. Liu, and Q. Liu, *J Macromol Sci Phys*. **48**, 309-317 (2009)
69. F.J. Buchanan, *Degradation rate of bioresorbable materials: Prediction and evaluation*, 2008, Elsevier Science (2008)
70. M. Arroyo, M.A. Lopez-Manchado, and F. Avalos, *Polymer*. **38**, 5587-5593 (1997)
71. M.A.L. Manchado, J.B.L. Torre, and J.M. Kenny, *Polym Eng Sci*. **40**, 2194 (2000)
72. D. Hull, and T.W. Clyne, *An introduction to composite materials*, 1996, Cambridge University Press (1996)
73. R.F. Gibson, *Principles of composite material mechanics*, 2011, Taylor & Francis (2011)
74. H.N. Dhakal, Z.Y. Zhang, and M.O.W. Richardson, *Compos Sci Technol*. **67**, 1674-1683 (2007)
75. L.V.J. Lassila, T. Nohrström, and P.K. Vallittu, *Biomaterials*. **23**, 2221-2229 (2002)
76. Y. Wan, Y. Wang, X. Xu, and Q. Li, *J Appl Polym Sci*. **82**, 150-158 (2001)
77. M.A. Slivka, and C.C. Chu, *J Biomed Mater Res A*. **37**, 353-362 (1997)

Figure Caption

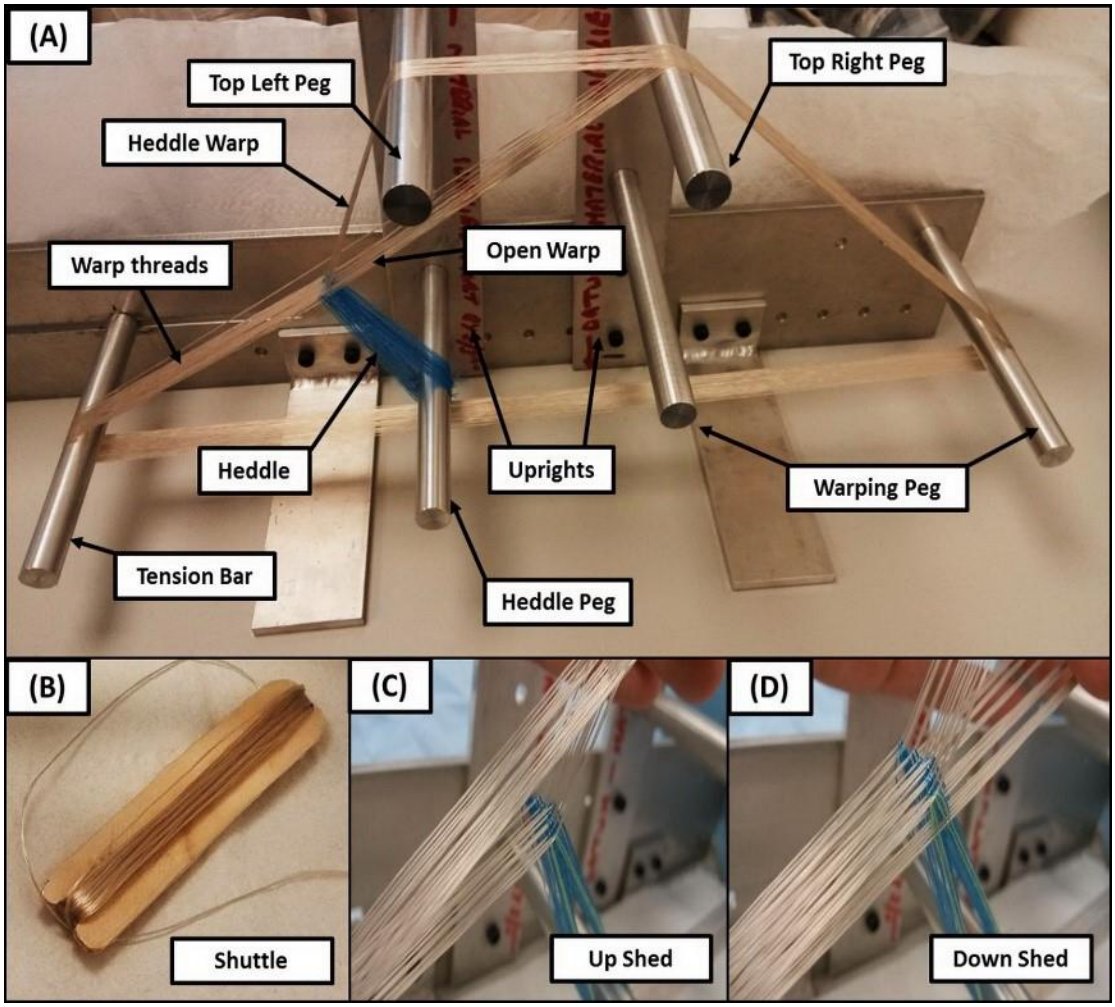

Figure 1: The image of Inkle loom for weaving textile of phosphate glass fiber (A); the image of shuttle (B) and the two types of shed during textile weaving (C and D).

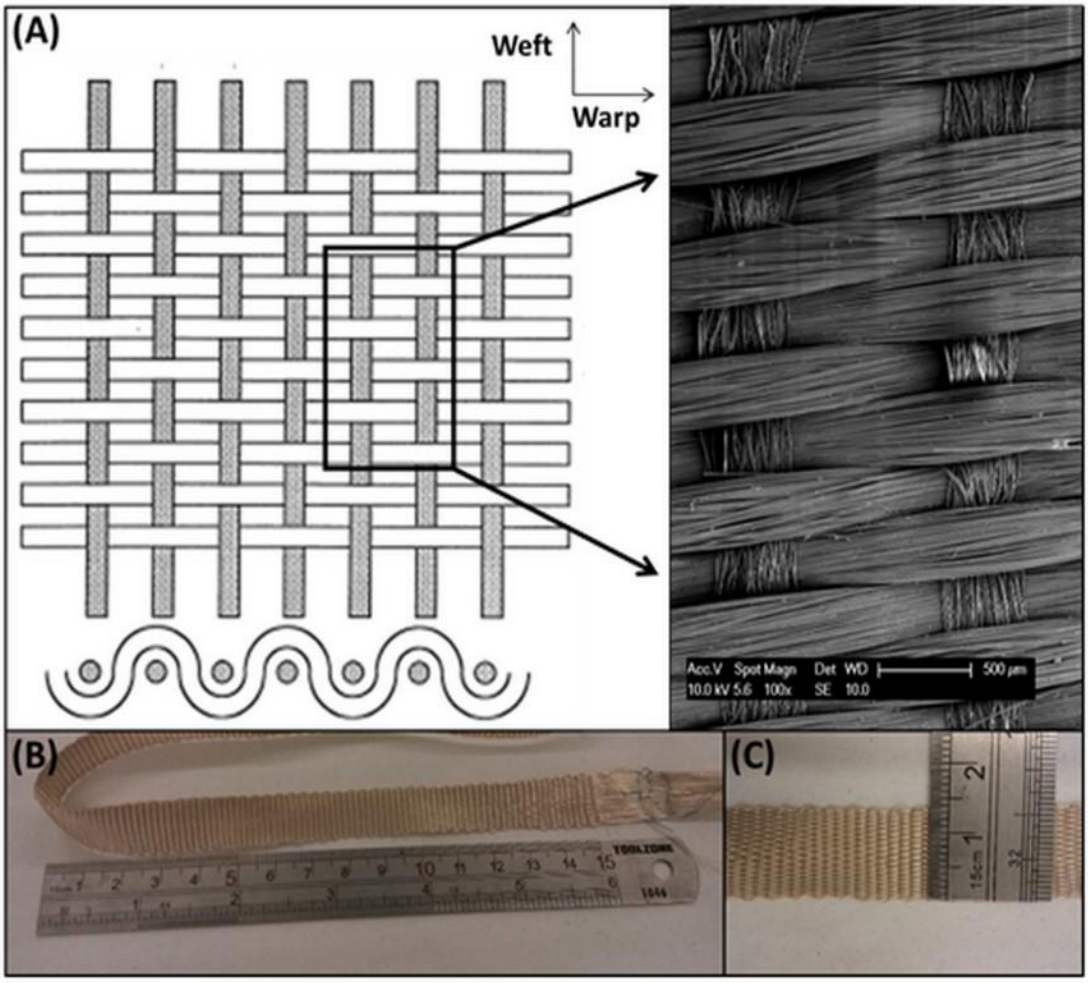

Figure 2: Schematic description of plain woven fabric structure and image from scanning electron microscopy (A); the image of textile woven by using yarns of phosphate glass fiber (B & C).

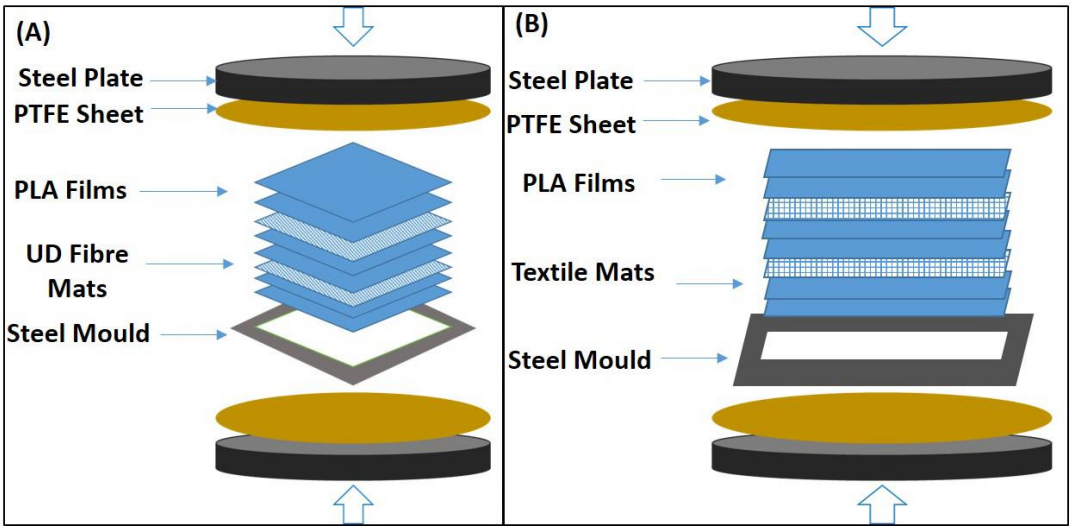

Figure 3: Schematic diagram of (A) unidirectional yarn reinforced composite (UD-C) and 0 ⁄90 ° lay-up composite (0/90-C) manufacture; (B) textile reinforced composite (T-C) manufacture.

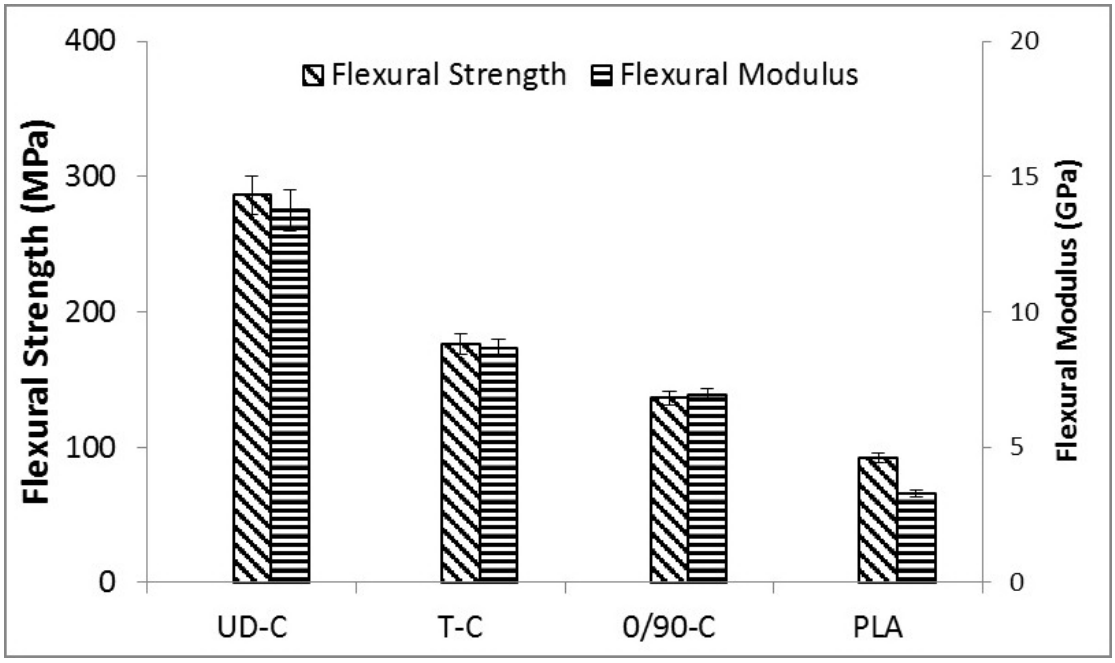

Figure 4: Initial flexural strength and flexural modulus of textile reinforced composite (T-C), 0 ⁄90 ° lay-up composite (0/90-C), UD composite reinforced with yarn (UD-C) and neat PLA plate.

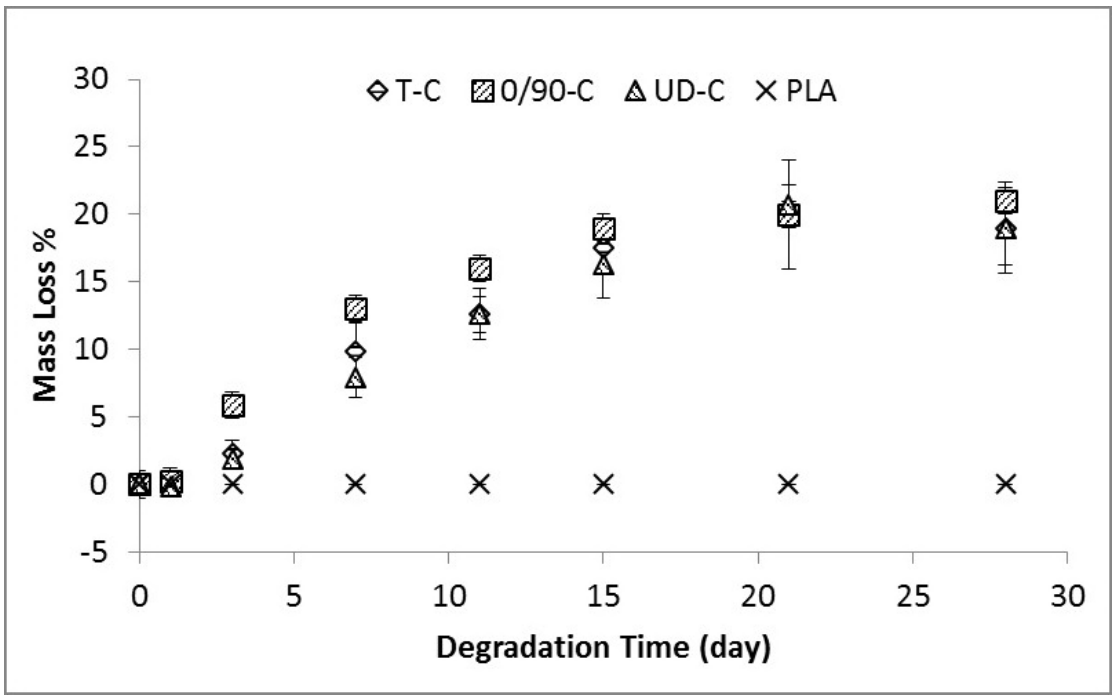

Figure 5: Mass loss of unidirectional yarn reinforced composite (UD-C), textile reinforced composite (T-C), 0 ℃/90 ° lay-up composite (0/90-C), and neat PLA plate, over degradation time in PBS at 37 ℃.

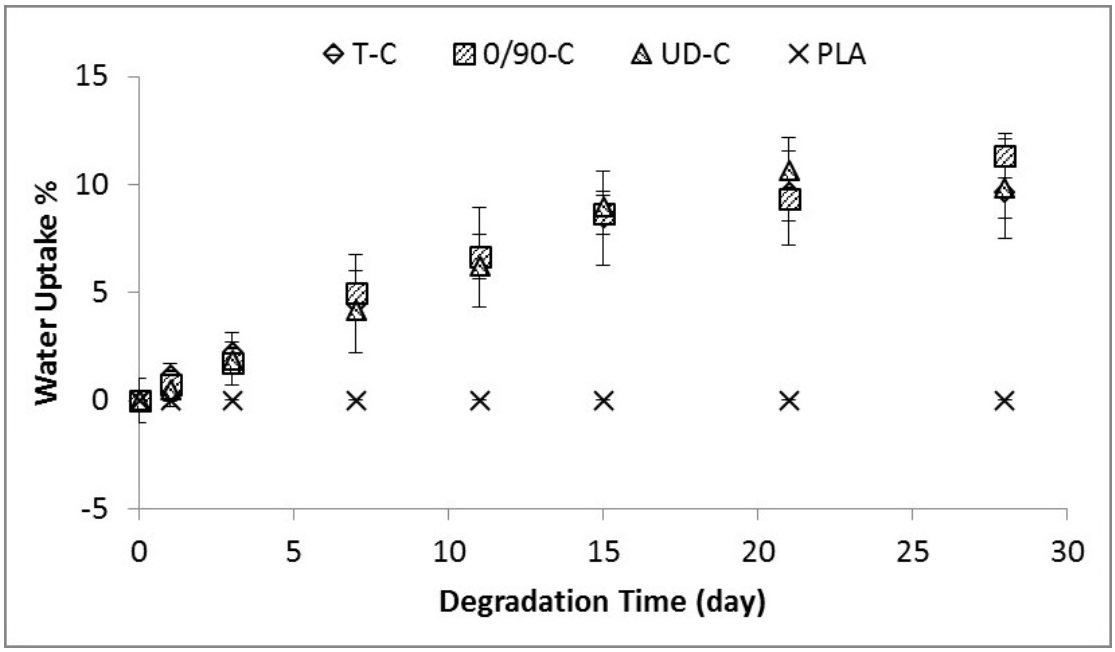

Figure 6: Water uptake weight percentage of textile reinforced composite (T-C), 0 ⁄90 ° lay-up composite (0/90-C), UD composite reinforced with yarn (UD-C) and neat PLA plate, over degradation time in PBS at 37 ℃.

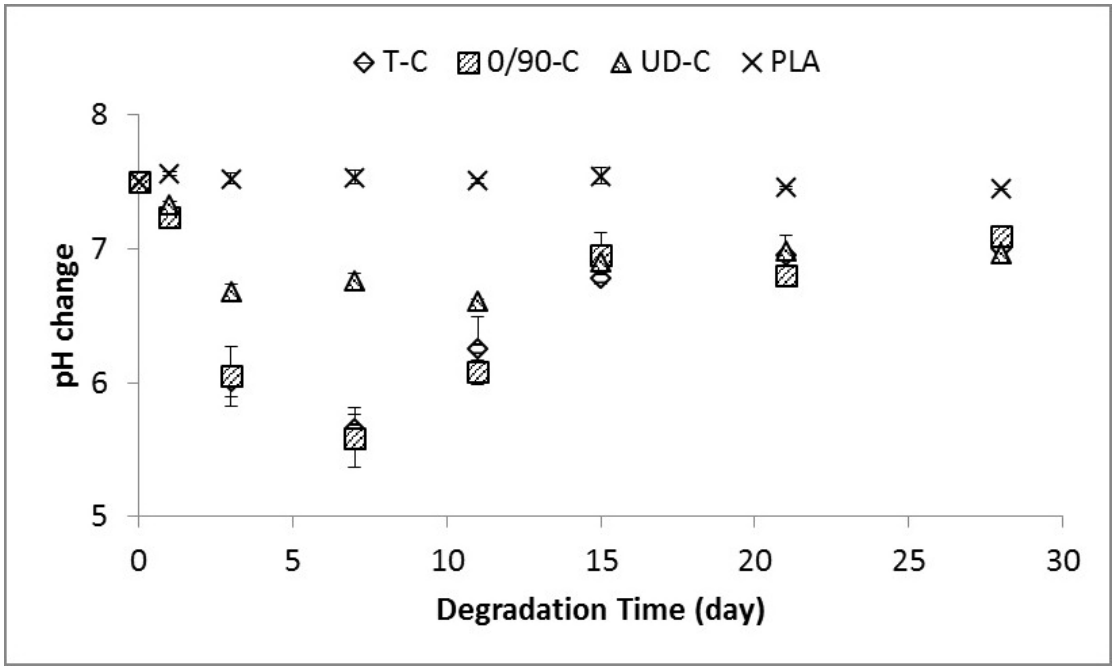

Figure 7: The pH change of textile reinforced composite (T-C), 0 ⁄90 °lay-up composite (0/90-C), UD composite reinforced with yarn (UD-C) and neat PLA plate, over degradation time in PBS at 37 ℃.

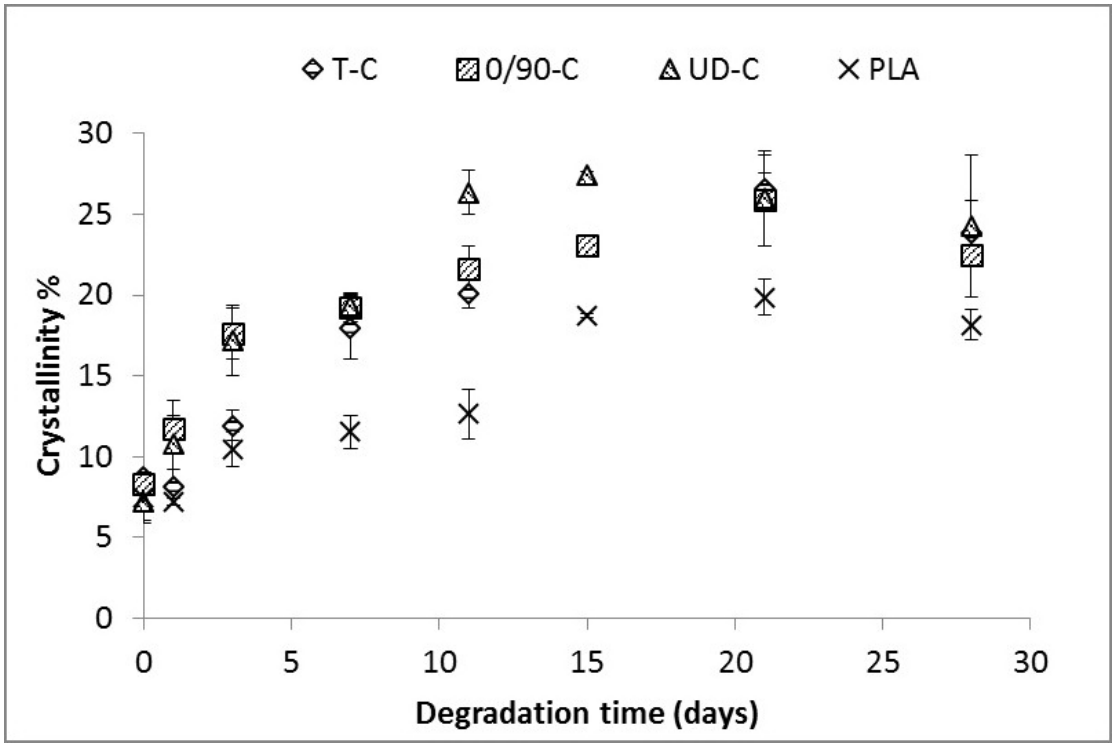

Figure 8: Degree of matrix crystallinity of textile reinforced composite (T-C), 0 ⁄90 ° lay-up composite (0/90-C), UD composite reinforced with yarn (UD-C) and neat PLA plate, over degradation time in PBS at 37 ℃.

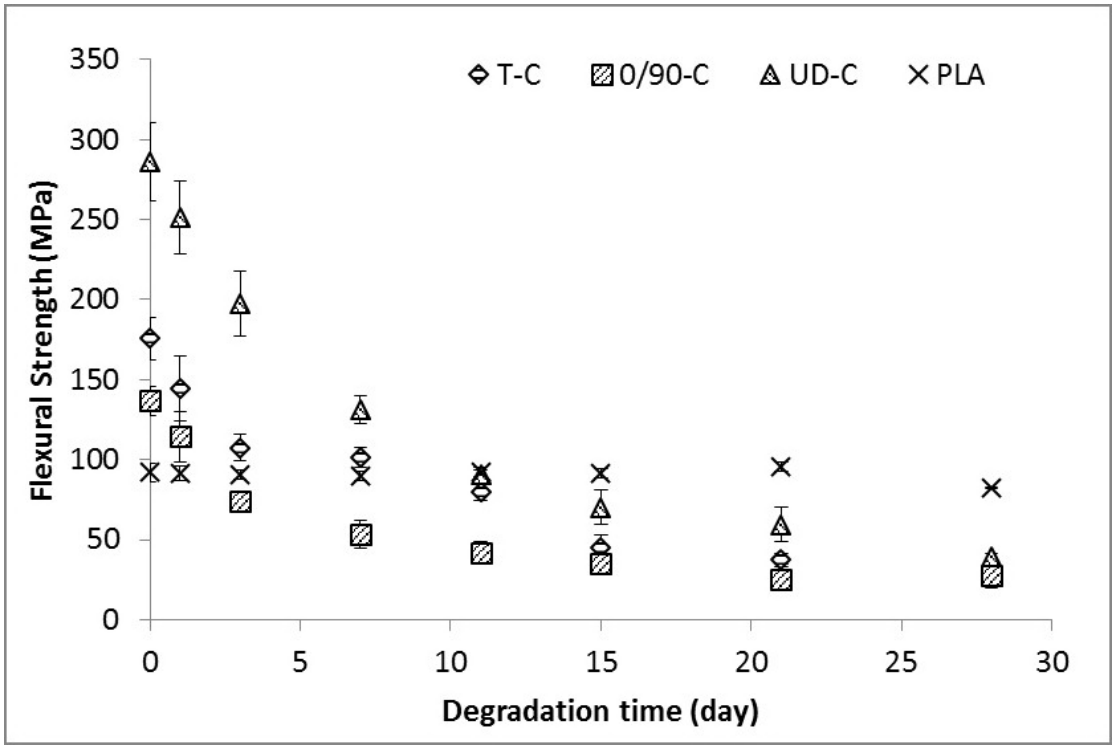

Figure 9: Flexural strength variation for textile reinforced composite (T-C), 0 ⁄90 °lay-up composite (0/90-C), UD composite reinforced with yarn (UD-C) and neat PLA plate, over degradation time in PBS at 37 ℃.

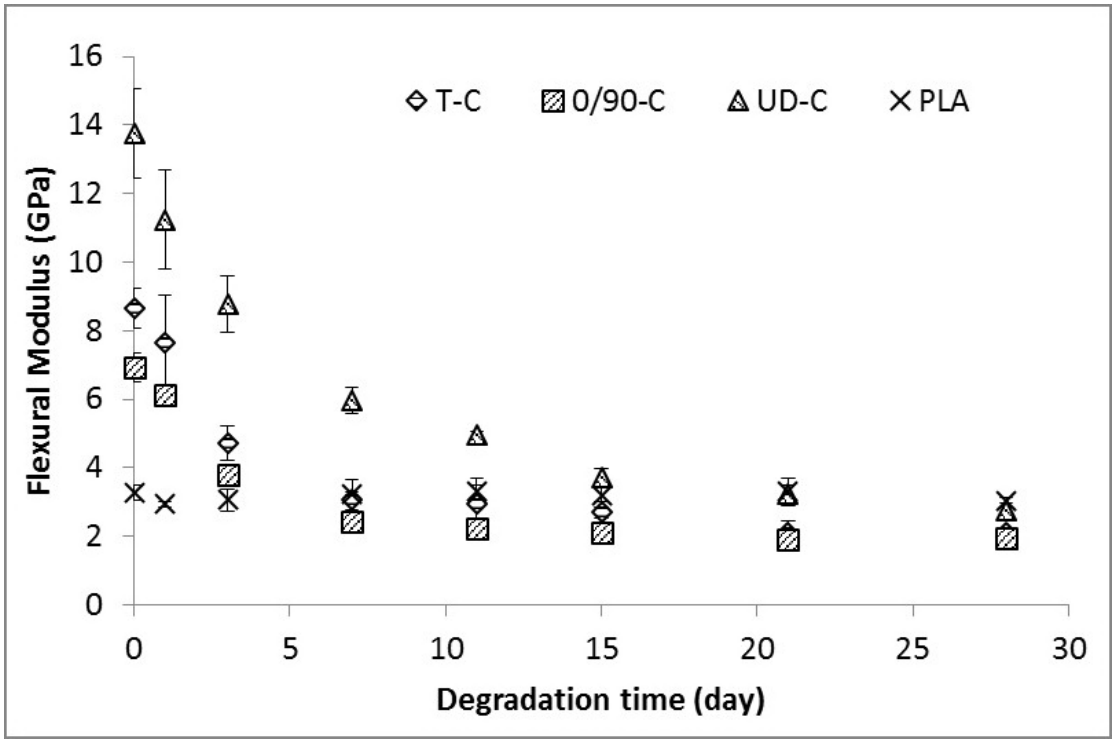

Figure 10: Flexural modulus variation for textile reinforced composite (T-C), 0 ⁄90 ° lay-up composite (0/90-C), UD composite reinforced with yarn (UD-C) and neat PLA plate, over degradation time in PBS at 37 ℃.

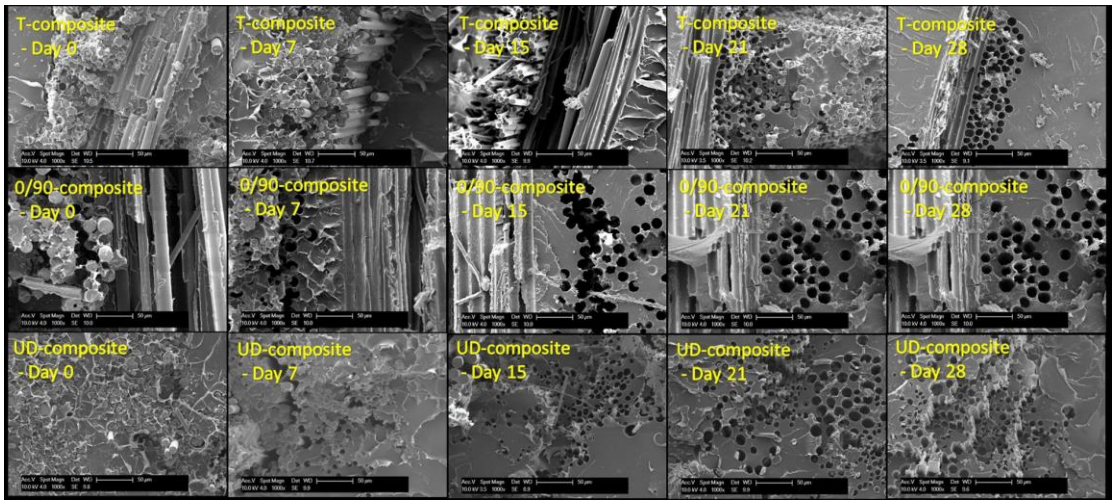

Figure 11: SEM images of fracture surfaces of textile reinforced composite (T-C), 0 ⁰/90 ° lay-up composite (0/90-C) and UD composite reinforced with yarn (UD-C), during degradation in PBS at 37 ℃.

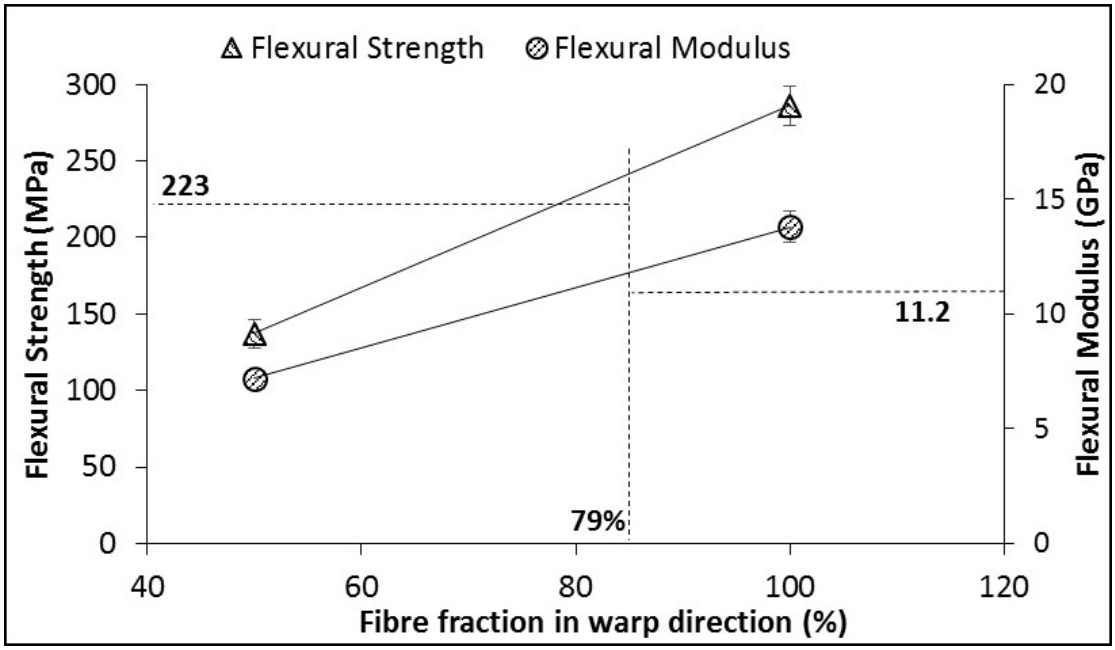

Figure 12: The variation prediction of mechanical properties with changing fiber fraction in warp direction, for unidirectional fiber mat reinforced composite (20% Vf), where (FS) is flexural strength and (FM) is flexural modulus.

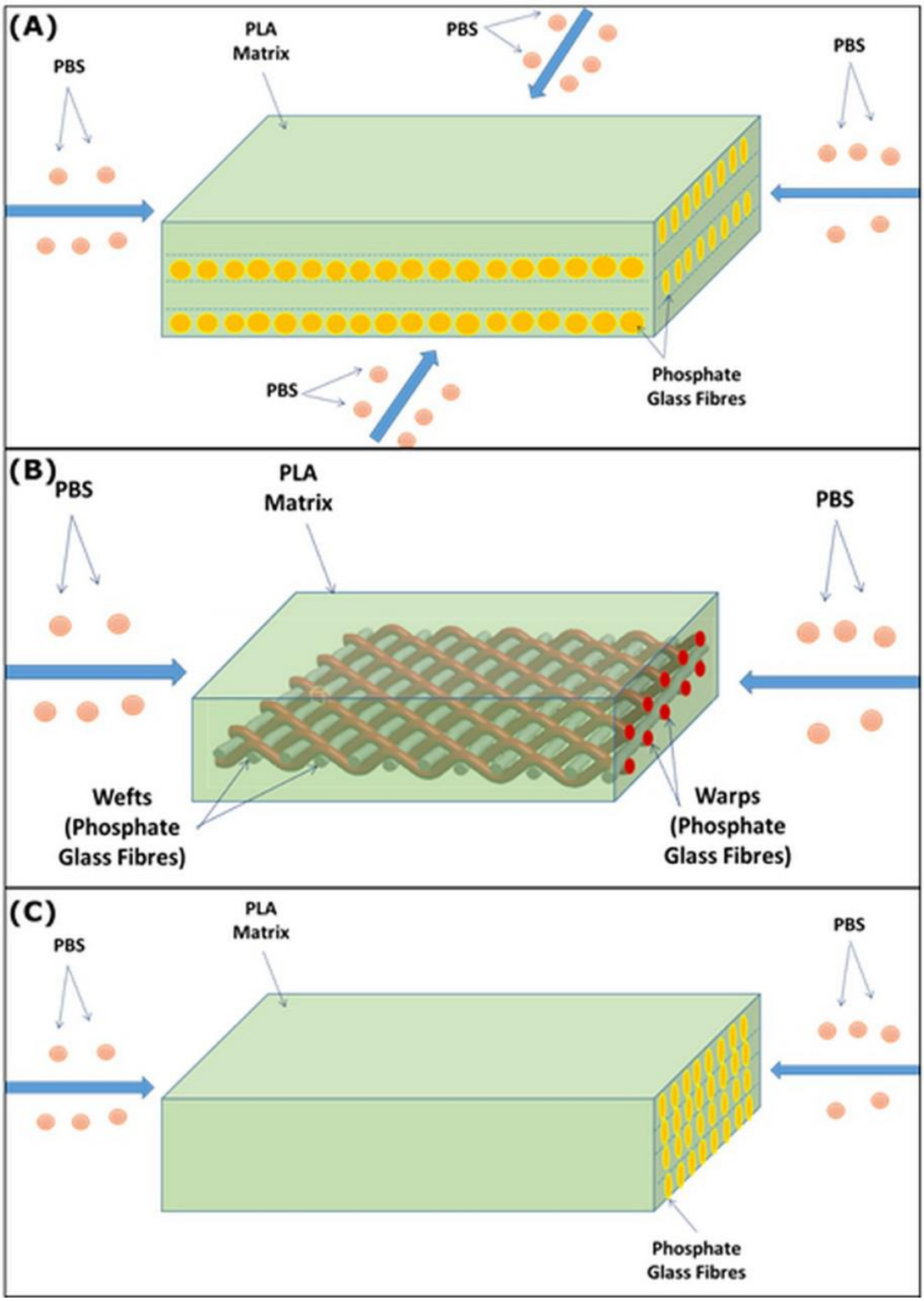

Figure 13: Degradation mechanism of 0/90-C (A), T-C (B) and UD-C (C) with open ends in PBS at 37 ℃.

Table Caption

Table 1: Geometry Parameters of the PGF textiles.

Pattern	Warp density (yarns/cm)	Weft density (yarns/cm)	Fabric Thickness mm
Plain Weave	22.7 ±0.2	6.1 ±0.2	0.362 ±0.013

Table 2: The sample description and fiber volume fraction of unidirectional composite (UD-C), textiles reinforced composite (T-C) and 0 ⁰/90 ° lay-up composite (0/90-C).

Sample Code	Sample Description	Fibers in warp direction	Target fiber volume fraction (%)	Experimental fiber volume fraction (%)
UD-C	Non-crimp laminate	100%	20	22 ± 2
0/90-C	Non-crimp laminate	50%	20	22 ± 3
T-C	Plain weave	79%	20	21 ± 1